Peer-reviewed version available at *Quaternary* **2018**, *1*, 30; doi:10.3390/quat1030030

Type of the Paper (Review)

The Potential of Speleothems from Western Europe as Recorders of Regional Climate: a Critical Assessment of the SISAL Database

Franziska A. Lechleitner [1]*, Sahar Amirnezhad-Mozhdehi[2], Andrea Columbu[3], Laia Comas-Bru[2], Inga Labuhn[4], Carlos Pérez-Mejías[5], and Kira Rehfeld[6]

[1] Department of Earth Sciences, University of Oxford, South Parks Road, Oxford OX1 3AN, UK; franziska.lechleitner@earth.ox.ac.uk
[2] UCD School of Earth Sciences, O'Brien Science Centre West, University College Dublin, Belfield, Dublin 4, Ireland; sahar.amirnejad@gmail.com (S.A.M.), laia.comasbru@ucd.ie (L.C.-B.)
[3] Department of Biological, Geological and Environmental Sciences, University of Bologna, Via Zamboni 67, 40126 Bologna, Italy; andrea.columbu2@unibo.it
[4] Institute of Geography, University of Bremen, Germany; inga.labuhn@geol.lu.se (ORCID 0000-0003-3755-5264)
[5] Department of Geoenvironmental Processes and Global Change, Pyrenean Institute of Ecology (IPE – CSIC), Avda. Montañana 1005, 50059 Zaragoza, Spain ; cperez@ipe.csic.es
[6] Institute of Environmental Physics, Ruprecht-Karls-Universität Heidelberg, Im Neuenheimer Feld 229, 69210 Heidelberg, Germany; krehfeld@iup.uni-heidelberg.de

* Correspondence: franziska.lechleitner@earth.ox.ac.uk

Abstract: Western Europe is the region with the highest density of published speleothem $\delta^{18}O$ ($\delta^{18}O_{spel}$) records worldwide. Here we review these records in light of the recent publication of the Speleothem Isotopes Synthesis and Analysis (SISAL) database [1]. We investigate how representative the spatial and temporal distribution of the available records is for climate in Western Europe, and review potential sites and strategies for future studies. We show that spatial trends in precipitation $\delta^{18}O$ are mirrored in the speleothems, providing means to better constrain the factors influencing $\delta^{18}O_{spel}$ at a specific location. Coherent regional $\delta^{18}O_{spel}$ trends are found over stadial-interstadial transitions of the last glacial, especially in high altitude Alpine records. Over the Holocene, regional trends are less clearly expressed, due to lower signal-to-noise ratios in $\delta^{18}O_{spel}$, but can potentially be extracted with the use of statistical methods. Overall, this first assessment highlights the potential of the European region for speleothem palaeoclimate reconstruction, while underpinning the importance of knowledge of local factors for a correct interpretation of $\delta^{18}O_{spel}$.

Keywords: SISAL database, speleothem, cave, oxygen isotopes, Western Europe, palaeoclimate

1. Introduction

Speleothems (secondary cave carbonates) are a widely used archive for the reconstruction of past terrestrial climate, and particularly for the investigation of high resolution climate variability, owing to their often exceptional chronological control [2,3]. The first version of the SISAL database (SISAL_v1) contains 376 speleothem records from across the globe [1]. About a quarter of these records (92) are from Western Europe, making it the region with the highest density of published speleothem datasets worldwide [1]. This paper reviews these records within the wider (palaeo-)climatic context of Western Europe, with the objective to identify and promote the potential of cave sites in the region for future palaeoclimate studies.

While early studies on Western European speleothems principally focused on their availability for temperature reconstruction using $\delta^{18}O$ of the carbonate [4,5], it was quickly recognised that $\delta^{18}O_{spel}$ is driven by a complex interplay of regional and site-specific factors, such as moisture source and

circulation dynamics, amount of precipitation, dripwater residence time in the overlying karst, cave temperature and ventilation dynamics, and potential kinetic effects during carbonate deposition [6,7]. Because of the filtering effect of the soil-karst system, the $\delta^{18}O_{spel}$ signal is usually strongly attenuated compared to precipitation $\delta^{18}O$, and affected to varying degrees by local noise [8]. This is particularly pronounced at mid-latitude sites and over the Holocene, when ranges in $\delta^{18}O_{spel}$ are typically small (average standard deviation of Western European $\delta^{18}O_{spel}$ in SISAL_v1 is 0.36‰) and reflect only moderate climate shifts. Over glacial-interglacial timescales, changes in the seasonality of precipitation and stationarity of climate patterns need to be considered as additional external drivers for variability in $\delta^{18}O_{spel}$ [9,10]. These, along with the fact that the climatic significance of a given speleothem-based record depends on the local climate, geology, hydrology, and vegetation, underpins the importance of interpreting speleothem records in their specific context. Western Europe possesses the highest density of Global Network of Isotopes in Precipitation (GNIP; [11]) stations worldwide, which provide information on climatic drivers of precipitation $\delta^{18}O$ in the region. Moreover, many cave sites are well studied, with continuous, high-resolution multiannual cave monitoring time series, and a good understanding of local climatic conditions. Monitoring data from caves and their surface environment provide a basis for understanding speleothem growth conditions in a specific setting (e.g., [12–16]). These present-day observations are enormously useful to delineate and characterize processes influencing speleothem geochemistry, and of critical importance for the calibration of recent speleothem records against meteorological data.

Given the almost unique ability of speleothems to provide high-resolution palaeoclimate records with tight chronological control, they are powerful archives for examining changes in climate variability and modes, and thus refine the picture obtained by other palaeoclimate archives. Focusing on Western Europe, where a large amount of palaeoclimate records from both speleothems and other archives is available, provides an opportunity to disentangle changes in mean climate state and variability.

Here we provide an overview of climate in Western Europe, before describing the available data in SISAL_v1 [1]. This study is focused at highlighting the potential of this new database for reconstructing regional trends in $\delta^{18}O_{spel}$, as well as identifying common issues encountered with speleothem records from this region.

2. Study Region and Climate

We define Western Europe roughly as the region between 11 and 16°E, and 36 and 71°N, based on political borders, and subdivide it into Southern Europe (< 45°N; Iberian Peninsula, Southern France, Italy except the alpine region), Northern Europe (> 45°N; Germany, Northern France, Belgium, Netherlands, Scandinavia), and the Alpine region (Austria, Switzerland, Italian Alps; Figure 1). Soluble lithologies, notably carbonates and evaporites, are present throughout the region, with the exception of most of Scandinavia, Northern Germany and the Netherlands, and parts of the Iberian Peninsula (Figure 1).

The present-day climate is characterised by strong spatial heterogeneity, and climate conditions become increasingly continental moving eastward from the Atlantic Ocean, as a result of predominant westerly moisture transport [17–19]. A latitudinal gradient is also present between the temperate-humid climate of Northern Europe and the seasonally arid climate of the Mediterranean region. These spatial gradients are reflected in the regional patterns of precipitation $\delta^{18}O$, and are predominantly related to the continental effect, with lower $\delta^{18}O$ due to progressive rainout and Rayleigh distillation with increasing distance from the Atlantic coast [8,20]. Deviations from this trend are found in Southern Europe, where the influence of water vapour from the Mediterranean Sea can lead to higher $\delta^{18}O$ values [21], and the Alpine region, where the altitude effect lowers precipitation $\delta^{18}O$ [20,22].

The most important driver of interannual climate variability is the North Atlantic Oscillation (NAO), which describes the distribution of atmospheric masses between the Arctic and the subtropical Atlantic [23]. Variations in the NAO strongly influence winter surface temperatures, precipitation patterns, and storminess in the North Atlantic realm and in Western Europe [23–25],

and modulate precipitation $\delta^{18}O$ [26–31]. On top of shifts in NAO polarity, changes in the location and geographical extension of the NAO's centres of action can occur, in particular related to the influence of other modes of climate variability in the North Atlantic region (e.g., the East Atlantic and Scandinavian patterns [32–34]). In the Mediterranean region, precipitation is largely controlled by the Western Mediterranean Oscillation (WeMO), understood as an East-West dipole of sea-level pressures between the Azores High and the Ligurian Low [35].

Regional and temporal variability in climate conditions are challenging with regards to the interpretation of palaeoclimate records, which are limited spatially and by temporal resolution and chronological accuracy. Thus, the potential of a large database of speleothem records lies in the possibility of extracting regional climate patterns from local responses at individual cave sites.

3. Western European Records in SISAL_v1

3.1. Spatio-temporal coverage and regional potential

In total, 146 published speleothem isotope records have been identified in Western Europe. Almost a hundred of these records (80 stalagmites, 7 flowstones, and 5 composites) from 41 caves are currently included in SISAL_v1 [1], with 11 records from the British Isles, 24 from Southern Europe, 22 from Northern Europe, and 35 from the Alpine region (Figure 1, Table 1).

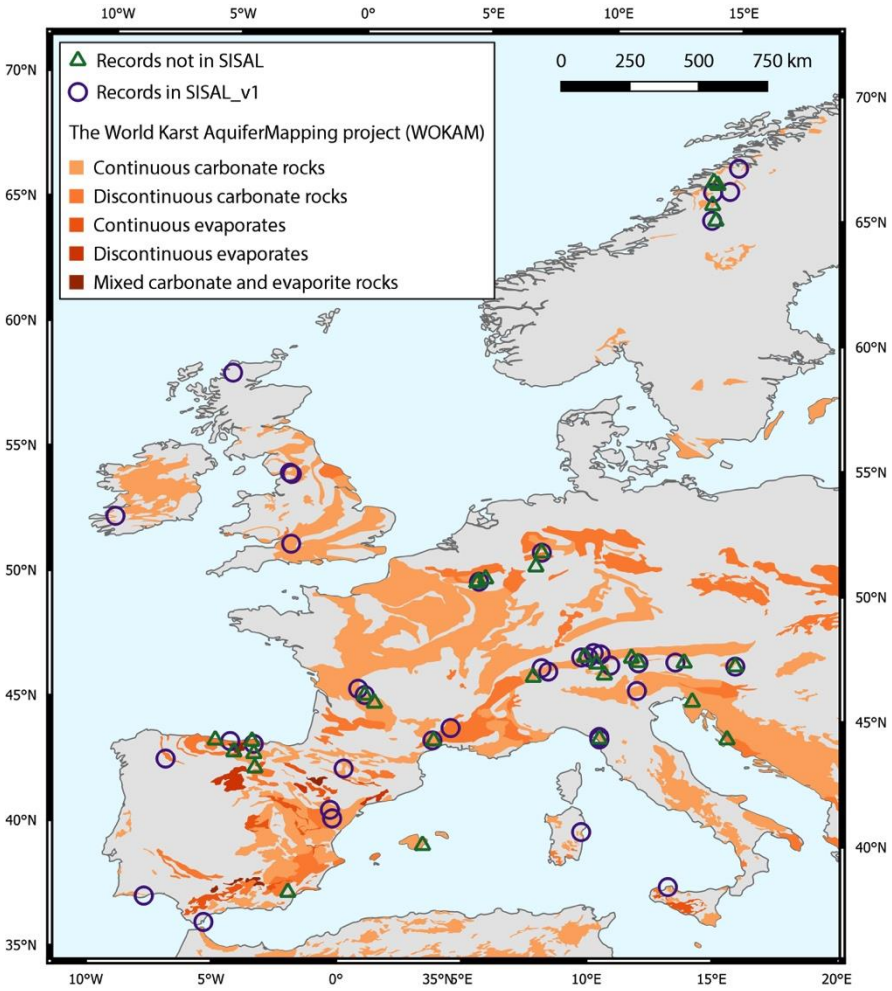

Figure 1. Map showing distribution of carbonate and evaporite rocks in Western Europe, provided by the World Karst Aquifer Mapping project (WOKAM, [36]). Green triangles indicate study sites in the region identified by the SISAL working group, while purple circles show the sites included in SISAL_v1. This map also shows sites that are not included in this study, as they were attributed to the Eastern European region.

Regional distribution of records with respect to the occurrence of soluble lithologies (carbonate and evaporite rocks) is patchy, in particular in central France and Germany, Eastern central Spain, and central-Southern Italy, where few records are published. While these lithologies do not necessarily contain caves and speleothems, these regions are potential targets for future speleothem-based palaeoclimate investigations. However, many sites in the region are protected, either due to the rich speleothem decorations or the presence of archaeological remains, requiring minimal sampling impact and close collaboration with other researchers and/or local caving communities.

Temporal coverage of the Western European records in SISAL_v1 reaches back to ~400 ka, with stalagmite CC-1 from Antro del Corchia in Italy providing the longest record (~265 kyrs, i.e., kilo-years, including growth stops; [37], Figure 2). Note that, in this study, ka BP is defined as thousand years before present, with the present referring to 1950 CE. The majority of the records however only cover the Holocene, with 8 speleothems deposited during the last millennium (Figure 2B). Temporal coverage of speleothem records beyond the Holocene steadily decreases with increasing age, with 17% of all records starting to grow during the Last Glacial period (~12 – 80 ka), 15% during Marine Isotope Stage 5 (MIS 5; ~80 – 135 ka), and 10% before MIS 5. The average length of the records is ~16 kyrs, including growth interruptions (min: ~50 years; max: ~265 kyrs; median: ~6.7 kyrs). Many records (33%), especially the longest ones, contain at least one hiatus (Figure 2). The longest uninterrupted record, stalagmite CC-5 from Antro del Corchia, Italy, covers ~80 kyrs [38]. The average chronological resolution over all records is 17 years, gradually decreasing with record length/antiquity (Figure 2). Some records have seasonal (e.g., Gib04a from St. Michaels Cave, Gibraltar; [64]) or annual resolution (e.g., ER76 from Ernesto Cave, Italy; [40]), but others only provide multi-decadal and centennial information (e.g., CC-1 from Antro del Corchia, Italy; [63]). The vast majority of records deposited since the end of the Last Glacial Maximum (LGM; last 21 kyrs) have annual to multi-decadal resolution over most of their length (Figure 2B). A tendency to more speleothem growth during interstadials and interglacials is apparent, especially at high latitudes (Figure 2A), highlighting the dominance of temperature control on hydroclimate and vegetation/soil dynamics in this region.

Records not yet included in the SISAL database will improve the temporal coverage of the region, e.g., records from Scandinavia covering past interglacials [41–43] will shed light on the temperature control of speleothem growth at high latitudes (Figure 2). Nevertheless, a bias towards more recent post-LGM reconstructions is apparent in our assessment, mainly because speleothems suffer of natural attrition [44]; recent deposits are usually more numerous (e.g., less breakage) and/or more suitable for geochemical analyses (e.g., less weathered and chemically altered) than older materials. Additionally, there has been a strong interest of the community for very recent reconstructions that allow calibration with instrumental records. Given the almost unrivalled ability of speleothems to provide high resolution and precisely dated records of past terrestrial climate, this highlights the potential of the region for more speleothem records spanning further back in time. This would be particularly useful for time periods beyond the range of radiocarbon dating (~50 ka), where chronological control in other archives becomes increasingly tenuous.

Preprints (www.preprints.org) | NOT PEER-REVIEWED | Posted: 13 September 2018 doi:10.20944/preprints201809.0246.v1

Peer-reviewed version available at Quaternary 2018, 1, 30; doi:10.3390/quat1030030

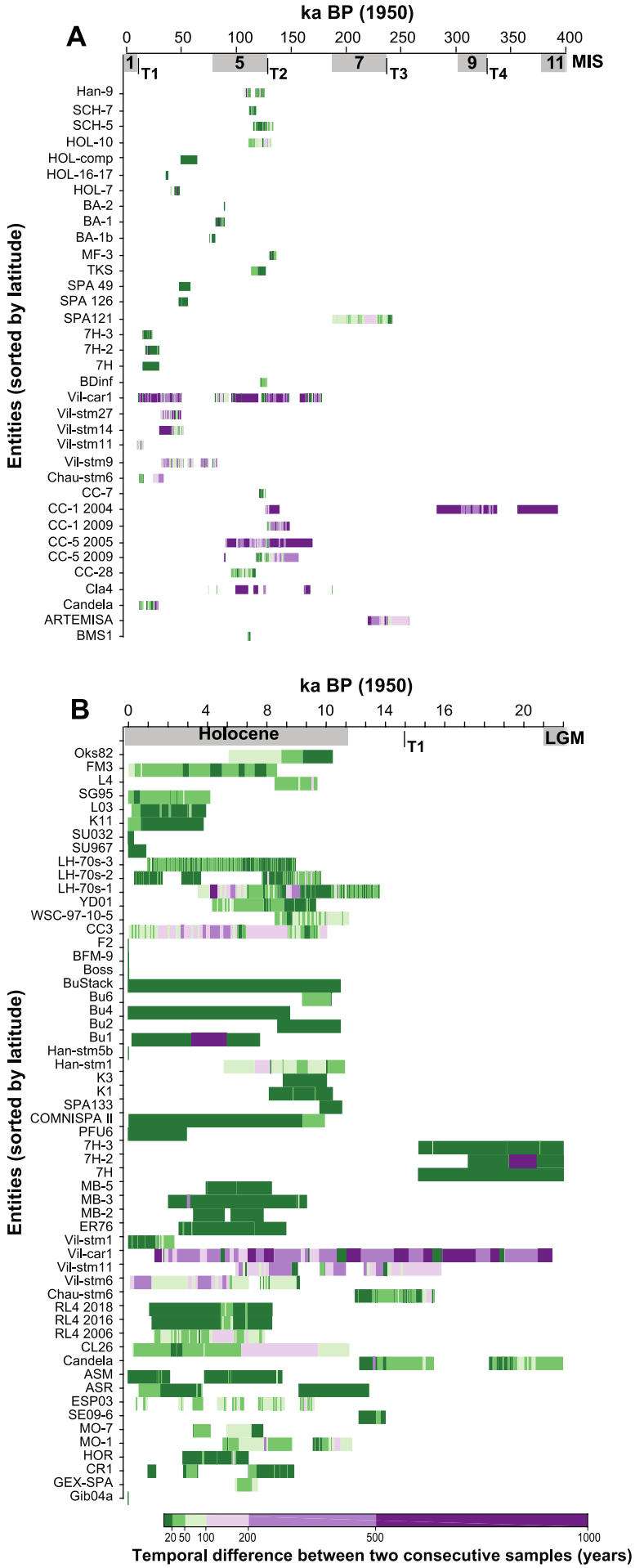

Figure 2. Temporal coverage of the Western Europe records present in SISAL_v1. A – records covering pre-Holocene time intervals. If a record extends into the Holocene, that part is shown in B. B – records covering the last 22 ka. MIS and glacial terminations (T) timings according to Lisiecki & Raymo (2005; [45]). Hiatuses in individual records are shown by blank spaces.

Entity_id	Entity name	SISAL site_id	site name	Country	latitude (°N)	longitude (°E)	Min. year (BP)	Max. year (BP)	Ref.
27	Vil-stm6	4	Villars	France	45.43	0.78	-43	8657	[1]
28	Vil-stm9	4	Villars	France	45.43	0.78	31437.91	82854.5	[46]
28	Vil-stm9	4	Villars	France	45.43	0.78	31437.91	82854.5	[47]
29	Vil-stm11	4	Villars	France	45.43	0.78	5361	15875	[48]
30	Vil-stm14	4	Villars	France	45.43	0.78	28892.68	52156.42	[47,49]
31	Vil-stm27	4	Villars	France	45.43	0.78	31340.9	49663.24	[46]
32	Vil-car1	4	Villars	France	45.43	0.78	1055	178002	[50]
33	Vil-stm1	4	Villars	France	45.43	0.78	-38	2333	[51]
50	LH-70s-1	8	Lancaster Hole	England	54.22	-2.52	3456.22	12717.56	[52]
51	LH-70s-2	8	Lancaster Hole	England	54.22	-2.52	261.86	9735.67	[2]
52	LH-70s-3	8	Lancaster Hole	England	54.22	-2.52	945.79	8462.88	[2]
70	BA-1b	15	Baschg	Austria	47.25	9.67	75492.44	80896.94	[53]
71	BA-1	15	Baschg	Austria	47.25	9.67	80982.06	89489	[53]
72	BA-2	15	Baschg	Austria	47.25	9.67	88609.98	89723.31	[53]
73	Han-stm1	16	Han-sur-Lesse	Belgium	50.12	5.19	4778	10949	[54]
74	Han-stm5b	16	Han-sur-Lesse	Belgium	50.12	5.19	-44	16	[55]
75	Han-9	16	Han-sur-Lesse	Belgium	50.12	5.19	106499.65	125343.05	[56]
85	SU967	21	Uamh an Tartair	Scotland	58.14	-4.93	-35	892	[57]
86	SU032	21	Uamh an Tartair	Scotland	58.14	-4.93	-53	271	[58]
95	FM3	26	Okshola	Norway	67	15	-47	7515.2	[59]
96	Oks82	26	Okshola	Norway	67	15	5006	10327.64	[59]
116	GEX-SPA	40	Excentrica	Portugal	37.1	-7.77	5329.36	6565.22	[60]
122	L4	46	Labyrintgrottan	Sweden	66.06	14.68	7347.5	9565.1	[61]

123	L03	47	Larshullet	Norway	66	14	130	3920.52	[62]
129	YD01	53	Pippikin Pot	England	54.21	-2.51	4205.58	9478.94	[52,63]
133	7H	55	Sieben Hengste	Switzerland	46.75	7.81	14620	29873	[64]
134	7H-2	55	Sieben Hengste	Switzerland	46.75	7.81	17137.17	29940.32	[64]
135	7H-3	55	Sieben Hengste	Switzerland	46.75	7.81	14639.45	23536.89	[64]
137	SG95	57	Soylegrotta	Norway	66	14	-43	4141.22	[41]
138	SPA12	58	Spannagel	Austria	47.08	11.67	60	5043	[65]
139	SPA70	58	Spannagel	Austria	47.08	11.67	4549	9894	[65]
140	SPA128	58	Spannagel	Austria	47.08	11.67	2520	6140	[65]
141	SPA127	58	Spannagel	Austria	47.08	11.67	2737	8449	[65]
142	COMNISPA II	58	Spannagel	Austria	47.08	11.67	-13	9930.6	[65]
150	WSC-97-10-5	66	White Scar	England	54.17	-2.44	7347.87	11190.74	[52,63]
154	SPA133	58	Spannagel	Austria	47.08	11.67	9636.5	10796.1	[65]
162	BDinf	73	Bourgeois Delaunay	France	45.67	0.51	121339	128151	[66]
166	Chau-stm6	77	Chauvet	France	44.23	4.26	11415	34183	[48]
180	Candela	87	Pindal	Spain	43.4	-4.53	11640.32	29339.98	[67,68]
182	Gib04a	89	New St Michael's	Gibraltar	36.13	-5.35	-53.6	2	[39,69]
192	Boss	96	Brown's Folly mine	England	51.38	-2.37	-47	32	[70,71]
193	BFM-9	96	Brown's Folly mine	England	51.38	-2.37	-47	21	[70,71]
194	F2	96	Brown's Folly mine	England	51.38	-2.37	-46	13	[70,71]

195	BMS1	97	Bue Marino	Italy	40.25	9.62	110207	112881	[72]
196	CC3	98	Crag	Ireland	52.25	-9.43	-47	10132	[73,74]
199	K1	100	Katerloch	Austria	47.08	15.55	7079.5	10324	[75]
200	K3	100	Katerloch	Austria	47.08	15.55	7786.62	10027.08	[75]
201	PFU6	101	Klapferloch	Austria	46.95	10.55	-47	2943.04	[76]
202	K11	102	Korallgrottan	Sweden	64.88	14	-55	3791.88	[77]
206	SCH-5	105	Schneckenloch	Austria	47.43	9.87	115340	134085	[78]
207	SCH-7	105	Schneckenloch	Austria	47.43	9.87	111588.73	118314.57	[53]
208	SE09-6	106	Seso	Spain	42.46	0.04	11616	12995	[79]
211	Cla4	108	Clamouse	France	43.71	3.55	74460	187405	[80]
212	CL26	108	Clamouse	France	43.71	3.55	142.33	11178.79	[73]
216	MO-1	109	Molinos	Spain	40.79	-0.45	4727	11334.76	[81]
217	MO-7	109	Molinos	Spain	40.79	-0.45	3253	6812	[81,82]
230	HOL-7	115	Hölloch im Mahdtal	Austria	47.38	10.15	40105	48664	[83]
231	HOL-16	115	Hölloch im Mahdtal	Austria	47.38	10.15	36701	63546	[83]
232	HOL-17	115	Hölloch im Mahdtal	Austria	47.38	10.15	35832	64934	[83]
233	HOL-18	115	Hölloch im Mahdtal	Austria	47.38	10.15	52509	57283	[83]
234	HOL-16-17	115	Hölloch im Mahdtal	Austria	47.38	10.15	35705	37578	[83]
235	HOL-comp	115	Hölloch im Mahdtal	Austria	47.38	10.15	49063	64498	[83]
236	HOL-10	115	Hölloch im Mahdtal	Austria	47.38	10.15	110844	131765	[78]
240	Bu1	117	Bunker	Germany	51.37	7.66	137	6644.9	[84]
241	Bu2	117	Bunker	Germany	51.37	7.66	7497.6	10723.5	[84]
242	Bu4	117	Bunker	Germany	51.37	7.66	-57.3	8162.8	[84]

243	Bu6	117	Bunker	Germany	51.37	7.66	8749	10258.2	[84]
244	BuStack	117	Bunker	Germany	51.37	7.66	-57.4	10723.5	[84]
248	ASR	119	Cueva de Asiul	Spain	43.32	-3.59	488.61	12160.96	[85]
249	ASM	119	Cueva de Asiul	Spain	43.32	-3.59	-62	7776.64	[85]
250	HOR	120	Ejulve	Spain	40.45	-0.35	2708.44	6071.82	[81]
251	ARTEMISA	120	Ejulve	Spain	40.45	-0.35	218975.67	257426.49	[10]
252	TKS	121	Entrische Kirche	Austria	47.16	13.15	113389.5	126889.04	[86]
255	MB-2	123	Milchbach	Switzerland	46.62	8.08	3248.65	6830	[87]
256	MB-3	123	Milchbach	Switzerland	46.62	8.08	1986.95	9025.84	[87]
257	MB-5	123	Milchbach	Switzerland	46.62	8.08	3889.71	7245.91	[87]
258	MB-6	123	Milchbach	Switzerland	46.62	8.08			[87]
260	MF-3	125	Schafsloch	Switzerland	47.23	9.38	130050	137390	[88]
261	SPA121	58	Spannagel	Austria	47.08	11.67	187290	242070	[89]
277	CR1	129	Grotta di Carburangeli	Italy	38.17	13.16	947.73	8373.72	[90,91]
279	ER76	131	Grotta di Ernesto	Italy	45.97	11.65	2511.48	7969.05	[40]
280	SPA_126	132	Kleegruben	Austria	47.08	11.67	47396	55966	[92]
281	SPA_49	132	Kleegruben	Austria	47.08	11.67	47816	58266	[92]
282	RL4_2006	133	Buca della Renella	Italy	44.08	10.21	1215.56	6928.36	[93]
283	RL4_2016	133	Buca della Renella	Italy	44.08	10.21	1150.37	7262	[94]
310	ESP03	143	Cova da Arcoia	Spain	42.61	-7.09	340	9440	[95]
313	CC-1_2004	145	Antro del Corchia	Italy	43.98	10.22	125432.63	393407.69	[37]
314	CC-5_2005	145	Antro del Corchia	Italy	43.98	10.22	88347	170549.44	[38]

315	CC-28	145	Antro del Corchia	Italy	43.98	10.22	95191.16	117497.82	[96]
316	CC-1_2009	145	Antro del Corchia	Italy	43.98	10.22	127997	148970	[97]
317	CC-5_2009	145	Antro del Corchia	Italy	43.98	10.22	117965	156957	[97]
318	CC-7	145	Antro del Corchia	Italy	43.98	10.22	121333	126805	[97]
381	RL4_2018	133	Buca della Renella	Italy	44.08	10.21	1024.11	7277.24	[3]
	Romeo		Cueva Rosa	Spain	43.43	-5.13	5294	8097	[98]
	C11		Cueva del Cobre	Spain	42.98	-4.37	77	2614	[99]
	GAR-01		La Garma	Spain	43.43	-3.66	10142	13757	[100]
	GAR-02		La Garma	Spain	43.43	-3.66	0	1000	[101]
	comp.		Kaite	Spain	42.94	-3.57	394	9569	[102]
	LV5		Kaite	Spain	42.94	-3.57	393	3885	[99]
	SLX1		Cueva Mayor	Spain	42.37	-3.51	62	1513	[99]
	Vil#10B		Villars	France	45.43	0.78			[103]
	Vil#1A		Villars	France	45.43	0.78			[103]
	VilGal#1B		Villars	France	45.43	0.78			[103]
	VilPlq-8		Villars	France	45.43	0.78			[103]
	Vil-stm24		Villars	France	45.43	0.78	102800	113600	[104]
	Fra-stm-6		La Faurie	France	45.13	1.18			[103]
	GC-01-05-02		Gitana	Spain	37.44	-2.02	58000	274000	[105]
	CCF-03-03-01		Cova de Cala Falco	Spain	39.5	3.3	48000	112000	[106]
	Cla-stm5		Clamouse	France	43.71	3.55	432000	611000	[104]
	Proserpine		Han-sur-Lesse	Belgium	50.12	5.19	-51	471	[107]
	PN-stm-95-5		Pere Noel	Belgium	50.13	5.16	1800	12900	[108,109]
			Hotton	Belgium	50.25	5.45	2750	11150	[108]

STAL-B7-1	B7	Germany	51.3667	7.6506	6196	12405	[110]
STAL-B7-5	B7	Germany	51.3667	7.6506	5850	8810	[110]
STAL-B7-7	B7	Germany	51.3667	7.6506	540	17230	[110]
STAL-AH-1	Atta	Germany	50.8	7.44	1763	2723	[111]
AH-1	Atta	Germany	50.8	7.44	860	8430	[112]
EXC-3	Beatus	Switzerland	46.38	7.49	100940	110000	[53]
EXC-4	Beatus	Switzerland	46.38	7.49	77450	107080	[53]
KC-1	Klaus-Cramer	Austria	47.26	9.52	54560	71940	[53]
	Hölloch im Mahdtal	Austria	47.38	10.15	1380	12690	[113]
COR-1	Antro del Corchia	Italy	43.98	10.22			[103]
CC-26	Antro del Corchia	Italy	43.98	10.22	750	11260	[114]
PFU-7	Klapferloch	Austria	46.95	10.55			[76]
PFU-8	Klapferloch	Austria	46.95	10.55			[76]
PFU-9	Klapferloch	Austria	46.95	10.55			[76]
HOT-1	Hötting Breccia	Austria	47.28	11.39	73900	98700	[115]
HOT-2	Hötting Breccia	Austria	47.28	11.39	70300	73800	[115]
SPA-4	Spannagel	Austria	47.08	11.67	265700	353900	[116,117]
SPA-59	Spannagel	Austria	47.08	11.67	52900	261400	[118]
SPA-12	Spannagel	Austria	47.08	11.67	15	2040	[119]
SPA-119	Spannagel	Austria	47.08	11.67	220500	226900	[116]
SPA-11	Spannagel cave	Austria	47.08	11.67	117000	202800	[120]
SPA-52	Spannagel	Austria	47.08	11.67	91100	204100	[120]

ENT-10	Entrische Kirche	Austria	47.16	13.15	114000	127000	[86]
SV-1	Grotta Savi	Italy	45.61	13.88	1325	16799	[121]
SG92-4	Soylegrotta	Norway	66	14	4500	8000	[4]
SG-92-2	Soylegrotta	Norway	66	14	320000	630000	[42]
SG93	Soylegrotta	Norway	66	14	253	10409	[5]
Ham-85.2	Hamarnes	Norway	66.42	14.02	4510	123000	[41]
K1	Korallgrottan	Sweden	64.88	14.15	6070	8629	[61]
PL-6	Laphullet	Norway	66.31	14.18	380000	502000	[43]
K-2	Katerloch	Austria	47.08	15.55			[122]
K-4	Katerloch	Austria	47.08	15.55			[122]
K-5	Katerloch	Austria	47.08	15.55			[122]
K-6	Katerloch	Austria	47.08	15.55			[122]
K-7	Katerloch	Austria	47.08	15.55			[122]
K-8	Katerloch	Austria	47.08	15.55			[122]
K-RZ6-072007	Katerloch	Austria	47.08	15.55			[103]
K-Top3-Cl	Katerloch	Austria	47.08	15.55			[103]

Table 1. Summary of all records currently included in SISAL_v1 for Western Europe and records identified but not yet included.

[1] D. Genty, unpublished work

[2] Atkinson, T.C., Hoffmann, D., unpublished

[3] R. Drysdale et al., unpublished

[4] Berstad et al., 1998

3.2. Dating Methods and Chronologies

Any palaeoclimatic interpretation hinges on the accuracy of the dating method and age modelling technique applied. Speleothems are known for their precise U-Th chronologies, but other dating methods (e.g., layer counting, radiocarbon) are applied as well, often in combinations. SISAL_v1 contains 1189 ages from Western European speleothems, 96% of which were obtained with the U-Th method. U-Th ratios were measured by Multi Collector-Inductively Coupled Plasma-Mass Spectrometry (MC-ICP-MS; 62% of the total) or Thermal Ionisation Mass Spectrometry (TIMS; 34% of the total). For the calculation of corrected ages, the most recent publications use the U-Th decay constants published in [123,124], while older datasets mostly refer to [125]. Other dating approaches such as ^{14}C analyses (e.g., [39,51]), layer counting (e.g., [40,126]) or approaches combining multiple methods each represent ≤ 2% of the total. The median two sigma (2σ) uncertainty related to single

ages is 1.2%, ranging between 0 and 131%; uncertainties of 0% refer only to the top of actively growing speleothems. The dating uncertainties vary according to the method used (Figure 3), with MC-ICP-MS dates being the most accurate (median 0.9%; min 0.2%; max 131%), followed by TIMS (1.5%; 0.3%; 67%), layer counting (2%; 0%; 13%), combination of multiple approaches (4%; 1%; 7%) and ^{14}C (17%; 4%; 42%). It should be noted that U-Th uncertainty increases in younger samples (i.e., last millennia), reflecting the difficulties in measuring the low radiogenic ^{230}Th content for recent speleothems [127] (Figure 3). For these young speleothems, other dating methods such as ^{14}C and layer counting might be more suitable and result in less overall uncertainty, as demonstrated by [39], who used a combination of ^{14}C measurements and counting of minima in seasonal stable carbon isotope ratio ($\delta^{13}C$) cycles to derive a precise chronology for a 53-year old stalagmite (Gib04a) from Gibraltar. For laminae counting, uncertainties are usually attributed after a series of independent counts (e.g., [71]), and offsets between band-counted and radiometric ages might occur if annual layers are missing (undercounting) and/or if intra-annual lamination is present (overcounting; [128,129]).

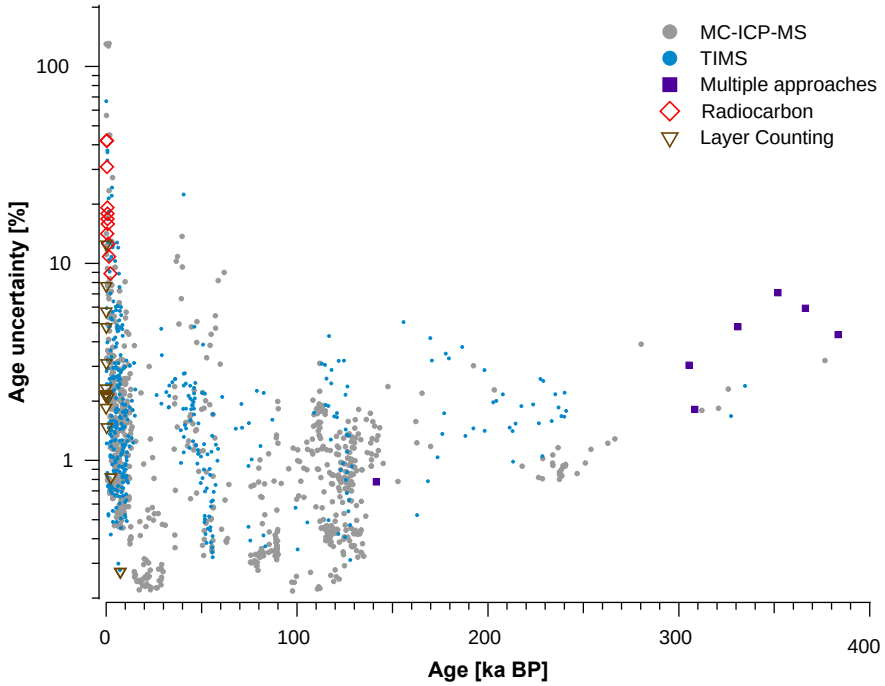

Figure 3. Dating methods, ages and age uncertainties. Shown are results in SISAL_v1 for MC-ICP-MS and TIMS U-Th dating, ^{14}C dating, laminae counting, and combinations of these methods (mostly U-Th or ^{14}C combined with laminae counting). Note that, for simplicity, ages with 0% uncertainty (i.e., top of actively growing speleothems) were excluded.

A vast variety of methods and algorithms is available to convert single dates to an age-depth model and, in most cases, calculate the propagation of age uncertainties through time. For Western European speleothems in SISAL_v1, the modelling procedures used are: StalAge (25%; [130]), linear interpolation (19%), Bayesian (not including OxCal, Bacon, BChron, and COPRA; 11%), polynomial fit (10%), OxCal (3%; [131]) and others or a combination of methods (30%). Here, "combination of methods" usually stems from the use of different dating techniques, e.g., ^{14}C and laminae counting in Gib04a from Gibraltar [39] or U-Th analysis and laminae counting in speleothems in Uamh an Tartair [126] and Larshullet Cave [62]. In our dataset, 13% of all ages were excluded from the final age-depth models in the original publications, mostly because they were not in the correct stratigraphic order and were thus considered unreliable. In radiometric dating, out-of-sequence anomalous ages can occur due to diagenetic phenomena affecting the carbonate fabric, and/or sources of error during sample preparation and analysis (e.g., cross-contamination, environmental contamination, spike calibration problems, [72,132–135]).

All age modelling protocols have their advantages and shortcomings [136], and emphasise different aspects of chronology development. In many cases, the age model for a single speleothem needs to take into account specific properties of the sample, e.g., petrographic and geochemical anomalies, and is thus to a certain extent subjective to the decisions of the user. This is important to ascertain the quality of the age-depth model for an individual speleothem, but might introduce biases. An updated age modelling technique intercomparison study appears timely with the publication of SISAL_v1 and would be helpful to determine common strengths and weaknesses in the models.

3.3. Availability of Environmental and Monitoring Data

Local climate and cave monitoring data are useful for the characterisation of the karst system and the processes acting on geochemical signatures recorded in speleothems. With sufficiently long time series of outside and in-cave temperature, and isotopic composition of precipitation and drip water, it is possible to estimate the extent to which $\delta^{18}O_{spel}$ records are representative of present-day external environmental signals. This is important, as fluid transfer through the karst system results in lagging, attenuation, or modification of the original precipitation signature. It must be noted, however, that this modern information needs to be carefully evaluated in the context of past climate, as the processes driving them might be temporally non-stationary and responding to climatic changes themselves (e.g., vegetation and soil cover, precipitation seasonality, changes in the temperature gradient between cave and exterior).

In Western Europe, temperature and precipitation data is widely available from meteorological stations for at least a few decades. Moreover, Europe has some of the longest meteorological records in the world, which go back to the 18th century (e.g., [137–139]). Gridded reanalysis or observational datasets provide continuous spatial coverage at high resolution since the late 19th century [140] and over 300 GNIP sites provide monthly or event-based measurements of isotopes in precipitation. Roughly 36% of these GNIP sites have been active for at least 10 years, and 57% for at least 5 years, providing an invaluable source of data to understand variability in precipitation and speleothem $\delta^{18}O$ (e.g., [88,89]). In-cave monitoring data, in contrast, is usually acquired within the context of specific speleothem studies, and is thus often limited by short-term, project-based funding or limited accessibility to the cave. Of the 174 cave systems included in the SISAL_v1 database, 66 have been monitored over at least one season (compared to 70 caves with no monitoring, and 38 where status of monitoring is unknown) and 22 of these are in Western Europe (53% of all caves in SISAL_v1 of the region).

3.4. Climate Controls on Speleothem Growth

In Western Europe, speleothem growth is promoted during interglacials and interstadials, when climate is warmer and more humid (Figure 2A). Presence/absence of growth and growth rate can both be powerful proxies for palaeoclimate conditions (e.g., [126,143,144]). The most straightforward climatic influence on speleothem growth is the presence of ice or permafrost above the cave, which prevent water percolation through the soil-karst system. This is observed at the Scandinavian cave sites, where speleothem growth is limited to interglacial time periods [43,59]. Conversely, evidence from high Alpine caves has shown that "subglacial" speleothem growth is possible if carbonate dissolution is promoted by sulphide oxidation, for instance seen in stalagmites from Milchbach Cave, Switzerland [87] and Spannagel Cave, Austria [116].

Changes in soil and vegetation activity are another mechanism influencing speleothem growth, as soil pCO_2 drives carbonate dissolution in the karst. Examples for such sites sensitive to changes in soil pCO_2 are Villars Cave in France, where cold phases during the last glacial are reflected by hiatuses in stalagmite Vil-stm9 [46], and Han-sur-Lesse Cave in Belgium, where stalagmite Han-9 stops growing after a period of drastic vegetation changes (shift to a more grass-dominated vegetation) and aridification synchronous with Greenland stadial 26 [56]. Milder stadial/glacial climate conditions at lower latitudes (e.g., Southern Italy and Southern Spain) appear to have allowed speleothem deposition at some sites (A. Columbu, personal communication), but these regions have

been scarcely targeted by researchers so far (Figure 1). Given the range of processes that can force speleothem growth cessation, a climatic interpretation of growth presence/absence and growth rates hinges on an assessment of potential site-specific controls.

3.5. Controls on $\delta^{18}O_{spel}$

A multitude of factors can influence $\delta^{18}O_{spel}$, from local effects such as cave temperature and karst infiltration dynamics, to processes driving precipitation $\delta^{18}O$ (air temperature, precipitation amount and seasonality, moisture source and circulation dynamics). This is especially pronounced at the mid-latitude sites of Western Europe, where competing forcings and a generally weaker climate control (especially during the Holocene) require detailed evaluation of the drivers of $\delta^{18}O_{spel}$.

The $\delta^{18}O_{spel}$ at sites included in SISAL_v1 is interpreted as dominantly reflecting air temperature (17 sites), precipitation amount (6 sites), moisture source (1 site), or a mixed signal of temperature and amount/moisture source (9 sites). The interpretation of $\delta^{18}O_{spel}$ remains unclear for 8 sites, as the original publications had a different focus.

A dominant temperature signal is found principally at high-altitude sites in the Alps (Baschg [53], Entrische Kirche [86], Grotta di Ernesto [40], Hölloch im Mahdtal [83], Katerloch [75], Kleegruben [92], Schafsloch [88], Schneckenloch [53,78]). At these sites, $\delta^{18}O_{spel}$ is understood to closely reflect precipitation $\delta^{18}O$, which is highly correlated to changes in air temperature during moisture condensation, with higher (lower) $\delta^{18}O$ reflecting warmer (colder) conditions (e.g., [83]). The authors of the original studies however emphasise that factors such as rainfall seasonality [53,75,86,88] or moisture source changes [78,83,89] play an additional role in the modulation of $\delta^{18}O_{spel}$, preventing a quantitative reconstruction of surface air temperatures. Interestingly, an opposite $\delta^{18}O$-temperature relationship (higher $\delta^{18}O_{spel}$ corresponding to lower temperature) has been reported for some alpine sites, most prominently Spannagel Cave, where $\delta^{18}O_{spel}$ has been interpreted in terms of variable dripwater sources (snowmelt water vs. rainfall), with more negative $\delta^{18}O$ values reflecting a larger contribution of melt waters and less negative $\delta^{18}O$ explained by a stronger share of meteoric waters due to glacier retreat during interglacials [120,145]. The high-latitude Scandinavian caves (Søylegrotta [41], Okshola [59], Labyrintgrottan [61], Korallgrottan [77] and Larshullet [62]) show the same reversed $\delta^{18}O$-temperature relationship, corroborated by temperature calibration studies [5,41], and are also explained by seasonally selective infiltration during snowmelt [59,61]. Only three sites at lower altitudes report a dominant temperature effect on $\delta^{18}O_{spel}$ (Han-sur-Lesse [56], Clamouse [73,80], and Crag [73]).

Sites with a dominant influence of precipitation amount on $\delta^{18}O_{spel}$ are widely spread throughout the region (Antro del Corchia [37,38,96,97], Buca della Renella [93,94], Bue Marino [72], Burgeois-Delaunay [66], Cueva de Asiul [85], Klapferloch [76]). In all these cases, higher (lower) $\delta^{18}O_{spel}$ is interpreted to reflect lower (higher) rainfall amount, as a consequence of isotopic depletion of precipitation during large storms [146]. Correlating speleothem $\delta^{18}O$ and carbon isotope ratios ($\delta^{13}C$) often helps discerning whether $\delta^{18}O_{spel}$ is driven by precipitation amount (e.g., [66,72]).

Several sites (Bunker [84], Cova da Arcoia [95], El Pindal [67], Grotta di Carburangeli [90], Molinos [81], Uamh an Tartair [57,58], Villars [46–50]) show a mixed signal of temperature and precipitation amount controls, which reduces their interpretability.

Moisture source is the third main driver for $\delta^{18}O_{spel}$ in Western Europe, as precipitation in these areas can originate from either the Atlantic or the Mediterranean, with the latter exhibiting higher $\delta^{18}O$ values [21,147,148]. Moreover, changes in atmospheric circulation patterns can lead to shifts in moisture trajectories and seasonality of precipitation at a site (e.g., [149]). These effects have been recognised as partially influencing many of the records in SISAL_v1, mostly as second-order trends (e.g., Baschg [53], Ejulve [10,81], Grotta di Ernesto [40], Schafsloch [88], Schneckenloch [53,78], Seso [79]). The composite record from Sieben Hengste (7H) Cave, Switzerland, is the only one where $\delta^{18}O_{spel}$ was interpreted as principally reflecting changes between northerly and southerly moisture transport, informing on shifts in the meridional position of the North Atlantic storm track during the LGM [64].

Due to these different factors potentially influencing $\delta^{18}O_{spel}$ in Western Europe, other proxies are often needed to better constrain the palaeoclimatic interpretation of the records, e.g., $\delta^{13}C$ or trace element ratios, and their use should be promoted in the future. One possibility to quantitatively reconstruct the isotopic signature of the "parent" precipitation $\delta^{18}O$ is through fluid inclusion stable isotope analysis in speleothems [49,51]. Fluid inclusions provide a more direct record of precipitation $\delta^{18}O$ than speleothem calcite and allow the reconstruction of palaeo-temperatures when used in combination with calcite $\delta^{18}O$, if this has precipitated at isotopic equilibrium [150]. However, the resolution of fluid inclusion $\delta^{18}O$ measurements remains much lower than for $\delta^{18}O_{spel}$.

4. Regional Patterns in $\delta^{18}O_{spel}$ Records Through Time

4.1. Spatial Trends and Comparison to Observations

Quantitative comparison between SISAL sites and the GNIP interpolated precipitation data ([151], available at www.waterisotopes.org) reveals moderate correlation ($r^2 = 0.33$, 22 sites, under the assumption of full independence between sites), with clear deviation from the 1:1 line, specially for high latitude sites (Figure 4A). Converting the precipitation $\delta^{18}O$ values to "speleothem" $\delta^{18}O$ values, i.e., taking into account the water-calcite fractionation using the relationship described in Kim and O'Neil (1997) [152] and correcting for offset between VSMOW and VPDB, reduces the correlation slightly ($r^2 = 0.27$, 22 sites), but altogether brings the agreement between precipitation and $\delta^{18}O_{spel}$ slightly closer to the 1:1 line (Figure 4B). It is apparent from this comparison that high latitude SISAL sites are strongly offset from their corresponding precipitation $\delta^{18}O$ values and removing these sites from the comparison between SISAL and interpolated GNIP data improves the correlation considerably ($r^2 = 0.42$, 17 sites, Figure 4C).

The present-day spatial trends in $\delta^{18}O$ (Figure 5) reflect the dominant climatic processes reflected in precipitation $\delta^{18}O$ and provide the opportunity to establish "base lines" of $\delta^{18}O_{spel}$, to which high-frequency changes can be compared, as well as to check whether single isotope records might be anomalous within their regional climatic context [8]. On the whole, a very similar East-West trend in $\delta^{18}O$ is apparent for precipitation and speleothems (Figure 5), which reflects increasing rainout away from the Atlantic (continental effect, [20]). Smaller-scale trends, such as the high $\delta^{18}O$ values found in the circum-Mediterranean region, and the altitude effect apparent in the Alpine region, are mirrored by the SISAL data. Despite this good spatial agreement over Western Europe, discrepancies are apparent with respect to absolute $\delta^{18}O$ values, as seen in the 2‰ offset in the regression equations (Figure 4), for which the speleothem records in Figure 5 have been adjusted.

Preprints (www.preprints.org) | NOT PEER-REVIEWED | Posted: 13 September 2018 doi:10.20944/preprints201809.0246.v1

Peer-reviewed version available at Quaternary 2018, 1, 30; doi:10.3390/quat1030030

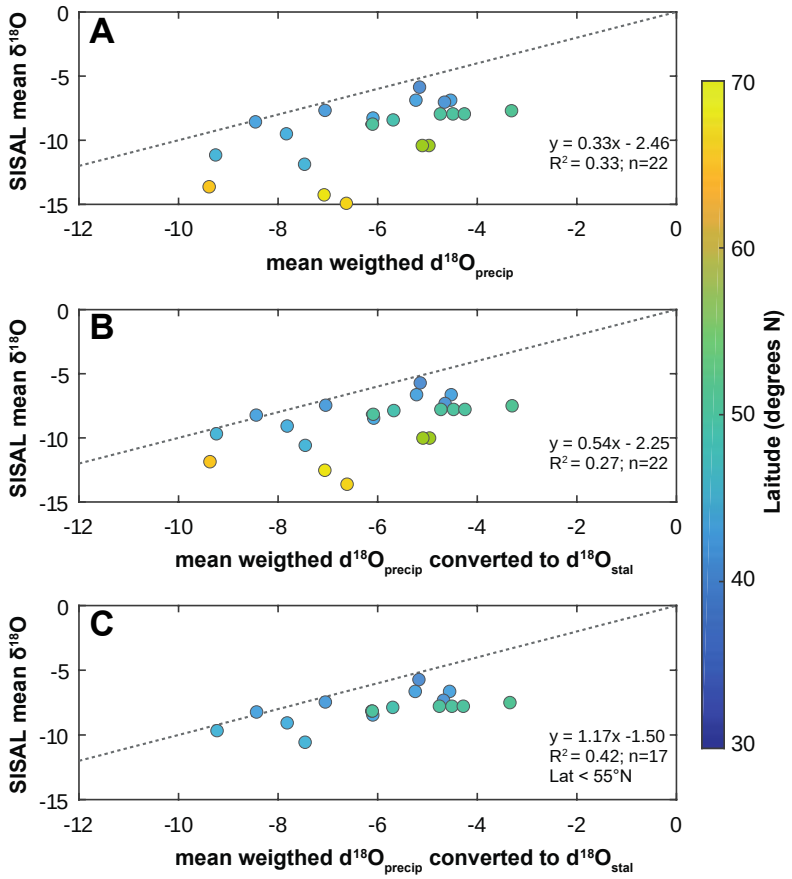

Figure 4. SISAL $\delta^{18}O$ vs. mean annual weighted precipitation $\delta^{18}O$ for the time period 1958-2015 from waterisotopes.org [151]. Colour coding indicates the latitude of the sites. A – Correlation between mean annual weighted precipitation $\delta^{18}O$ (in ‰ VSMOW) and $\delta^{18}O_{spel}$ in SISAL (in ‰ VPDB; n=22), as shown in Figure 5. Precipitation $\delta^{18}O$ was extracted at the locations corresponding to a SISAL site. B – Similar to A, but after converting precipitation $\delta^{18}O$ to calcite values using the equation in [152] for $\delta^{18}O$ water-calcite fractionation and converting from VSMOW to VPDB. C – Same as B, for latitudes between 30 and 55°N (n=17).

Local conditions are known to affect speleothem geochemistry and need to be taken into account when developing transfer functions for climate reconstruction. The isotopically effective recharge [7], related to the dominant infiltration season and the degree of mixing in the karst aquifer, can substantially affect the correlation between $\delta^{18}O_{spel}$ and precipitation $\delta^{18}O$ [142,153]. Small-scale variability in mountain climate that is not captured by the interpolation approach used for the GNIP data is likely the reason for the offset between SISAL sites and the GNIP data in the Alpine region and northern Scandinavia (Figure 5; [28]).

Preprints (www.preprints.org) | NOT PEER-REVIEWED | Posted: 13 September 2018 doi:10.20944/preprints201809.0246.v1

Peer-reviewed version available at Quaternary 2018, 1, 30; doi:10.3390/quat1030030

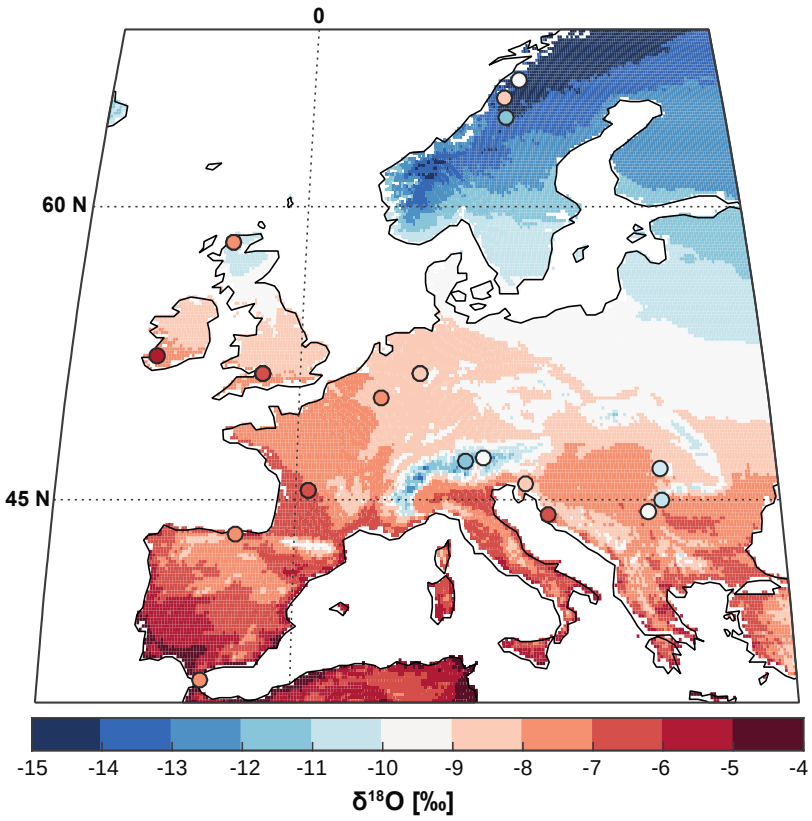

Figure 5. Comparison between mean annual weighted $\delta^{18}O$ data from waterisotopes.org (background map; [123]) and SISAL records (filled circles; n=18). The latter have been averaged over the period 1958-2017 and are shown at their corresponding cave locations. The SISAL records were not filtered to have a minimum number of data points. Note that the averages of the speleothem records have been offset by -2‰, based on the correlations in Figure 4.

4.2. Last Glacial Period

The SISAL_v1 database contains 24 records that cover the last glacial time period *sensu latu*, i.e., the period between 10 and 120 ka (Figure 6). Many records from high altitude alpine cave sites show a very clear response to millennial-scale forcing from the North Atlantic (e.g.; 7H, SPA 49, SPA 126, HOL-7, HOL-10, HOL-16-17, HOL-comp, BA-1, BA-1b, BA-2; Figure 6B). This strong synchronicity and similarity in the climatic response of the northern Alpine region and Greenland suggests a tight coupling between the two regions, which is likely related to the strong temperature control in these high altitude speleothems [83].

Speleothems from other cave sites in the region show a much less consistent pattern over the last glacial period, probably as a result of the complex interplay of processes affecting $\delta^{18}O_{spel}$ at mid-latitudes (Figure 6C). In some of these cases, the original authors used other geochemical proxies, such as $\delta^{13}C$, for the palaeoclimate interpretation. Stalagmites from Villars and Chauvet caves in France, for example, suggest a complex combination of temperature, precipitation amount and source changes affecting and muting their $\delta^{18}O_{spel}$, whereas $\delta^{13}C$ appears to be more sensitive to stadial-interstadial forcing. The authors interpret these rapid shifts in $\delta^{13}C$ as reflecting changes in soil CO_2 production, which is linked to temperature and humidity [46–48].

Preprints (www.preprints.org) | NOT PEER-REVIEWED | Posted: 13 September 2018 doi:10.20944/preprints201809.0246.v1

Peer-reviewed version available at Quaternary 2018, 1, 30; doi:10.3390/quat1030030

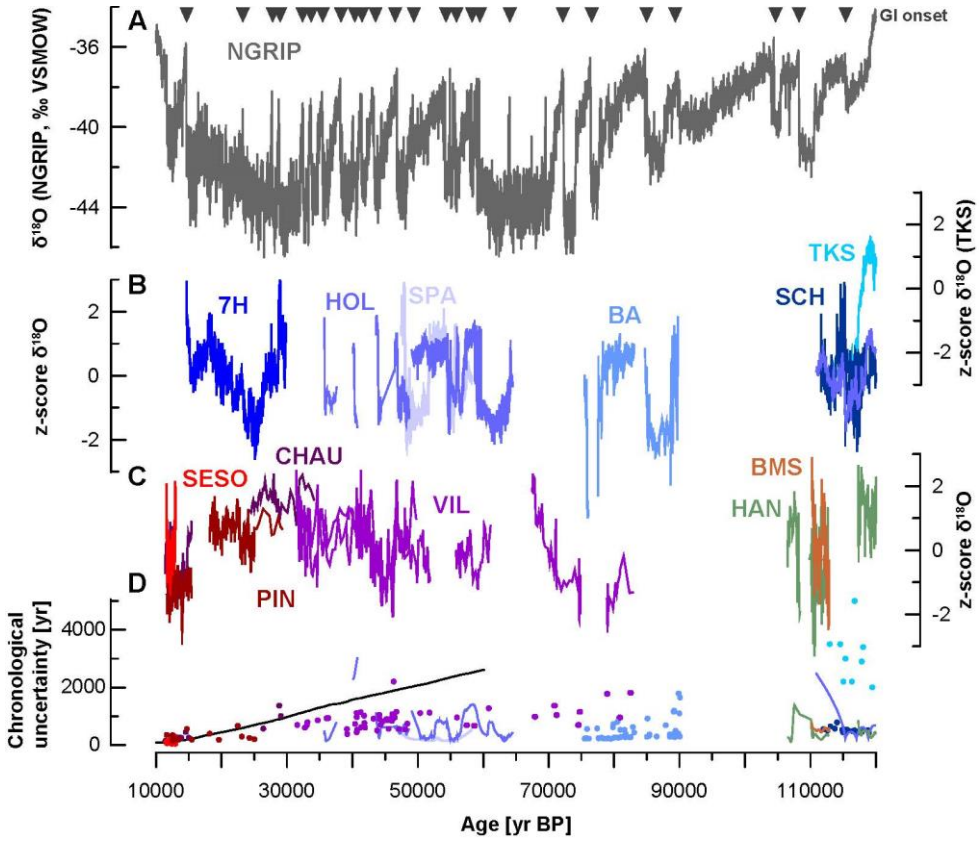

Figure 6. Examples of Western European records covering the last glacial period in SISAL_v1. To ease intercomparison of $\delta^{18}O_{spel}$, all records were normalised as z-scores. The onset of GIs is indicated by the grey triangles [154,155]. A – Greenland NGRIP ice core δ18O on the layer-counted GICC05modelext time scale for the last 60 kyrs, and extended further back on the ss09sea06bm time scale [155–157]. B – Records from the Alpine region (colour coded): 7H – Composite record from Sieben Hengste Cave, Switzerland [64], SPA – Stalagmites SPA 49 and SPA 126, Kleegruben Cave, Austria [92], HOL – Stalagmites HOL-7 and HOL-10, composite records HOL-16-17 and HOL-comp from Hölloch Cave, Austria [78,83], BA – Stalagmites BA-1, BA-1b, and BA-2 from Baschg Cave, Austria [53], SCH – Stalagmites SCH-5 and SCH-7 from Schneckenloch Cave, Austria [53,78], TKS – Flowstone TKS from Entrische Kirche Cave, Austria [86]. Note that TKS is shown on a different y-axis to ease visual comparison. C – Records from other parts of Western Europe (colour coded): SESO – Stalagmite SE09-6 from Seso Cave, Spain [79], PIN – Stalagmite Candela from El Pindal Cave, Spain [68,158], CHAU – Stalagmite Chau-stm6 from Chauvet Cave, France [48], VIL – Stalagmites Vil-stm9 and Vil-stm27 from Villars Cave, France [46,47], HAN – Stalagmite Han-9 from Han-sur-Lesse Cave, Belgium [56], BMS – Stalagmite BMS1 from Bue Marino Cave, Italy [72]. D – Chronological uncertainty of the records: speleothem U-Th ages are shown in colour coded dots. If available, the uncertainty of the age model is shown instead, as a more accurate measure of the time series uncertainty (lines). The black line indicates the maximum counting error of the layer-counted part of the ice core chronology [157].

4.3. Holocene Climate Variability

In our first assessment, we find no consistent regional trends in $\delta^{18}O_{spel}$ in SISAL_v1 records from Western Europe spanning the entire Holocene period. This is partly due to age modelling uncertainties and low temporal resolution in some records, which prevents the detection of climatic shifts in $\delta^{18}O_{spel}$ during periods with low signal-to-noise ratios. Although Holocene climate conditions are more stable than during the last glacial period, recent evidence suggests significant variability, challenging the notion of a "very stable Holocene" [159]. The 8.2 ka event, the most severe Holocene climate perturbation recorded globally, can be used as a benchmark to test the sensitivity of records for millennial-scale climate change. In SISAL_v1, 21 records from Western Europe cover the time

period around 8.2 ka, and nine of them were interpreted by the original authors as recording evidence for a climatic perturbation at that time (Figure 7). Another four show changes in their growth and petrography (i.e., hiatuses, erosional surfaces, changes in calcite fabrics) that can tentatively be related to climate change around 8.2 ka. For most of the records, however, chronological uncertainty and/or temporal resolution remain an issue, and the detailed structure and timing of the 8.2 ka event often cannot be resolved (Figure 7). As a result of the paucity of available datasets it is also not possible at this stage to assess any regional trends in the expression of the 8.2 ka event in stalagmites from Western Europe. Recent advances in analytical and sampling methods provide an opportunity for future studies to obtain more detailed insights into this event, both in previously sampled records and at new sites.

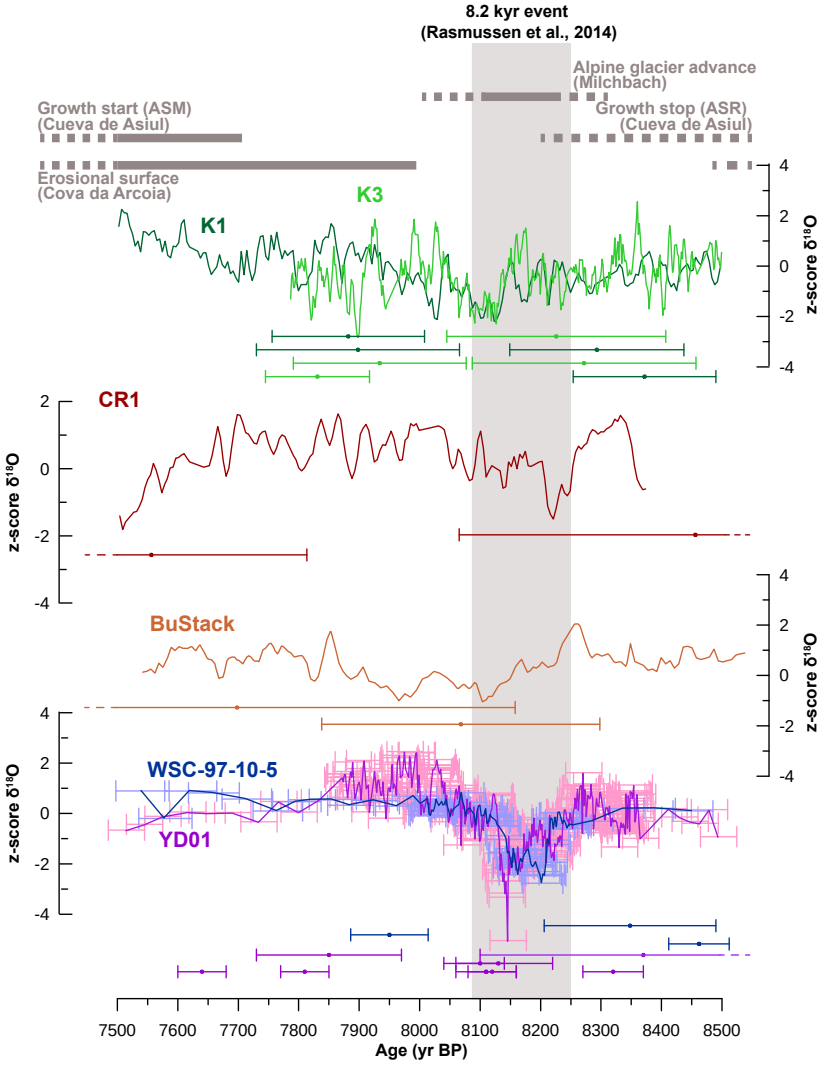

Figure 7. Examples of Western European records in SISAL showing evidence for a climatic perturbation over the 8.2 ka event. To facilitate intercomparison of $\delta^{18}O_{spel}$, all records were normalised as z-scores. The duration of the 8.2 ka event is shown with the grey bar [154]. K1, K2 – Stalagmites from Katerloch Cave, Austria [75], CR1 – Stalagmite from Grotta di Carburangeli, Italy [90], BuStack – Composite record from Bunker Cave, Germany [84], WSC-97-10-5 – Stalagmite from White Scar Cave, England [63], YD01 – Stalagmite from Pippikin Pot Cave, England [63]. Ages with respective 2σ uncertainties are shown below each record. For WSC-97-10-5 and YD01, the uncertainties of the age model are also shown (shaded error bars underlying the time series). Note that the uncertainty of the Bunker Cave composite record is likely smaller than suggested by the single U-Th ages, due to overlap of single stalagmite records, but this information was not available in SISAL_v1 [84]. Stalagmites with petrographic or growth rate evidence for a climatic event are shown in grey bars at the top: a glacier advance is suggested by petrographic changes in stalagmites from

Peer-reviewed version available at Quaternary 2018, 1, 30; doi:10.3390/quat1030030

Milchbach Cave, Switzerland [87], growth cessation/start around the event is recorded by stalagmites ASR and ASM from Cueva de Asiul, Spain [85], and an erosional surface is found in stalagmite ESP03 from Cova da Arcoia, Spain [95].

4.4. The Last Two Millennia

We evaluated the regional coherency of $\delta^{18}O_{spel}$ over the last two millennia using the data in SISAL_v1 by stacking all records covering at least 1/3 of the interval (-50– 2000 yr BP) at reasonable resolution (≥ 10 data points), and for which an age model is available. Nine records fulfil these requirements: stalagmite Vil-stm1 from Villars Cave, France [51]; stalagmite LH-70s-3 from Lancaster Hole, England (Atkinson, T.C. and Hoffmann, D., unpublished dataset); stalagmite FM3 from Okshola Cave, Norway [59]; stalagmite L03 from Larshullet Cave, Norway [62]; stalagmite SG05 from Soylegrotta Cave, Norway [41]; stalagmite CC3 from Crag Cave, Ireland [73]; flowstone PFU6 from Klapferloch Cave, Austria [76]; stalagmite CL26 from Clamouse Cave, France [73]; and stalagmite Bu4 from Bunker Cave, Germany [84]. After a Gaussian smoothing on a 100-year timescale was performed for all records, they were interpolated to 5-year timescales. For the stack, the unweighted average of all records was used, and no weighting based on location, correlation strength, or uncertainty was performed.

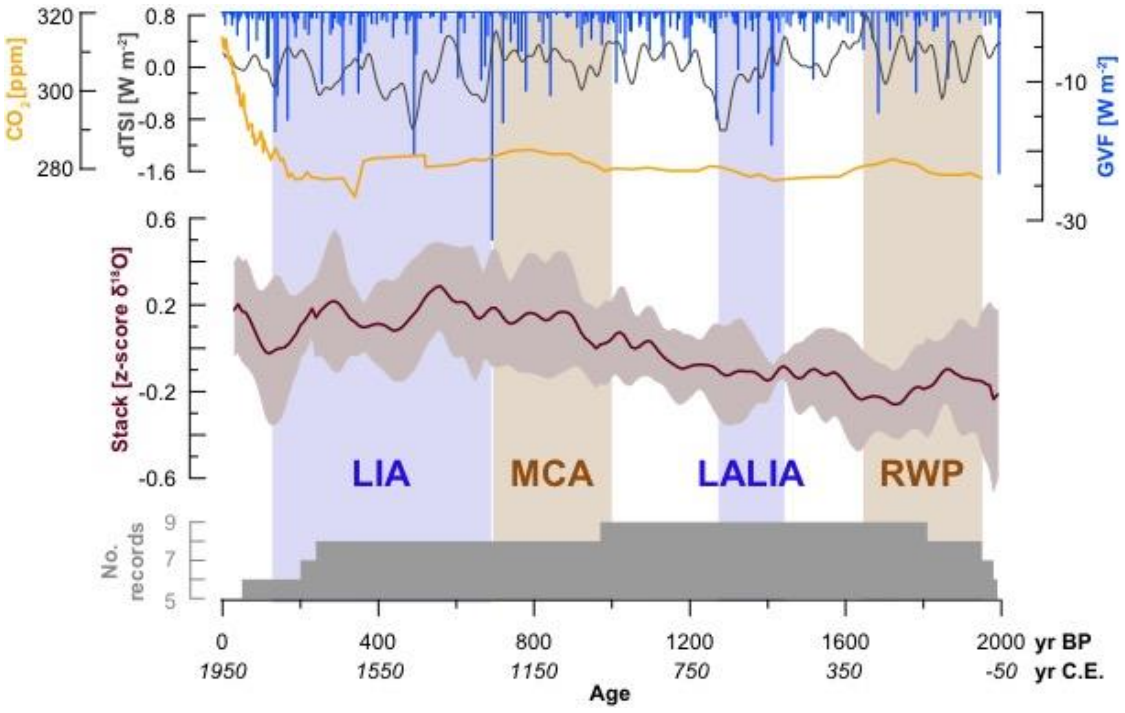

Figure 8: Stacked record of SISAL entities covering the last 2000 years, compared to Global Volcanic Forcing (GVF; [160]), solar forcing (total solar insolation anomalies, dTSI; [161]), and CO_2 concentrations from Antarctica's Law Dome record [162]. Important climate periods are indicated, and defined according to the following references: Little Ice Age (LIA; [163]), Medieval Climate Anomaly (MCA; [164]), Late Antique Little Ice Age (LALIA), and Roman Warm Period (RWP; [165]).

The stacked record for the last 2000 years shows a long-term trend towards more positive $\delta^{18}O_{spel}$ between 2000-550 yr, followed by a reversal and possibly a more oscillating behaviour (Figure 8). The reversal in the stack (trend toward lower $\delta^{18}O_{spel}$) at 550 yr falls within the Little Ice Age (LIA; [163]). However there is no clear indication of systematic changes in $\delta^{18}O_{spel}$ corresponding to the Roman Warm Period (RWP; [165]), the Late Antique Little Ice Age (LALIA; [165]), or the Medieval Climate Anomaly (MCA; [164]), periods of significant temperature change in Europe. This failure may reflect the high uncertainties related to the degree of noise in the single speleothem records, as well as the

Peer-reviewed version available at Quaternary 2018, 1, 30; doi:10.3390/quat1030030

different climate signals recorded by the individual speleothems. It is important to note that the stack captures the mean $\delta^{18}O_{spel}$ signal in Western Europe, and not a single climate process, e.g., temperature or precipitation amount. A screening of the records based on their response to climate was not possible at present, since most records are not calibrated against instrumental data. If more records that fulfil this requirement become available, a stack based on the recorded climate process might become feasible. In addition, future improvements of this procedure should tackle a regional assessment of the trends using a higher number of records and possibly including proxy data from other archives, checking correlations between nearby records, incorporating age uncertainties, and the integration of the signal's interpretation by the original authors.

5. Improvements to SISAL for Western Europe

Only 60% of the known records from Western Europe are in the SISAL_v1 database and the remaining records are widely distributed across Europe (Austria: 22, Belgium: 3, France: 7, Germany: 5, Italy: 3, Norway: 5, Spain: 9, Sweden: 1, Switzerland: 2). We have shown, for the current version of the database, that the speleothem records from Western Europe have potential to document some aspects of past climate change. However, it is clear that outstanding issues need to be addressed first, which in Western Europe can be summarised as i) improvement of temporal coverage, ii) improvement of spatial coverage, especially with records calibrated against modern climate conditions, and iii) a more comprehensive use of statistical approaches to extract underlying modes from spatially distributed records.

Overall, the paucity of records spanning beyond 22 ka presents an opportunity for future studies to target speleothems covering previous time periods, especially given their often more reliable U-Th chronologies at these time scales compared to ice cores and marine sediment records [10,166,167]. Climate variability over the last glacial and beyond remains poorly constrained, and speleothems could provide detailed information from vast range of different environments (coastal, continental, high altitude/latitude, etc.).

Records that contribute to improving our assessment of the spatial robustness of $\delta^{18}O_{spel}$ in Western Europe need to be calibrated against modern conditions, taking advantage of the GNIP network and climate model simulations. This is particularly important for the goals outlined by SISAL, as $\delta^{18}O$ is by far the most reported speleothem geochemical proxy, and the only one that has a direct parameter equivalent in climate model simulations with isotopic tracers. Instrumental and modelling data have recently allowed to define regions within Western Europe that are particularly suited for reconstructions of certain (hydro-)climatic conditions, especially with respect to spatio-temporal non-stationarities of the NAO [25,27,28]. In particular, variable sensitivities to the NAO have been implied for Central Europe, the Iberian Peninsula, the Baltic Sea, the British Isles, and the circum-Mediterranean region [28]. Record coverage in these areas is still patchy (Figure 1), and should be targeted by future efforts, ideally including long-term cave microclimate monitoring, assessment of local hydroclimate variability (through the isotopic analysis of precipitation samples from the cave site), and careful sampling practices.

Competing influences on $\delta^{18}O_{spel}$ and low signal-to-noise ratios at mid-latitude sites still prevent a quantitative interpretation of $\delta^{18}O$. As recently demonstrated by Deininger et al. [29], who used Monte Carlo based Principal Component Analysis on several $\delta^{18}O_{spel}$ records in the same region, sophisticated statistics methods can extract a common mode of climate variability from these datasets. Our approach of stacking different records is also useful to determine robust regional trends in a quantitative manner, but needs to be refined by future studies. Such statistical approaches hold great promise in the context of a large database like SISAL, and could be used to better constrain spatial trends in precipitation $\delta^{18}O$ over time, and improve our understanding of local and regional influences on $\delta^{18}O_{spel}$.

6. Future Directions

This first assessment of the Western European data compiled in the SISAL_v1 database highlights interesting spatial and temporal trends in stalagmite $\delta^{18}O$, but these will need to be validated and better constrained by future work on the database. Specifically, we encourage:

- Inclusion of missing records. This is crucial for the assessment of temporal and spatial coverage of speleothem records in Western Europe, and helps defining future target regions and time periods for new studies. This could be a starting point for revisiting sites and speleothems that have shown great sensitivity for climate reconstruction, but where resolution and/or chronological precision could be improved. It could also be of interest for a better definition of short-lived events such as the 8.2 ka event or the 4.2 ka event, and to improve chronological controls of speleothems previously dated with TIMS.
- Addition and use of other types of data. For example, fluid inclusion $\delta^{18}O$ measurements on speleothems would provide important direct information on past precipitation $\delta^{18}O$. Similarly, speleothem $\delta^{13}C$ data, already included in the database, should be evaluated, as many sites highlight its importance as (qualitative) proxy for soil activity and hydroclimate [40,46,71].
- Inclusion of more information about cave monitoring. The SISAL_v1 database only includes a yes/no/unknown entry for cave monitoring, which is often not sufficient when evaluating the extent of knowledge of modern cave conditions.

7. Conclusions

By assessing the speleothem data collected in the SISAL_v1 database for Western Europe, we describe regional trends in $\delta^{18}O$, and evaluate their potential for palaeoclimate studies. Western Europe has the largest number of published speleothem palaeoclimate records worldwide, many of which (> 60% of the identified records) are currently included in SISAL_v1. Moreover, climate conditions are well understood, due to the availability of a dense network of GNIP stations, some of the longest meteorological records worldwide, and global modelling and reanalysis datasets. This is a great advantage for the interpretation of $\delta^{18}O_{spel}$ records, which at mid-latitude sites is often difficult because of competing effects from precipitation and cave processes. We find that present-day spatial trends in $\delta^{18}O_{spel}$ from Western European caves generally mirror the trends in precipitation $\delta^{18}O$. Over the late Quaternary, site-specific noise in $\delta^{18}O_{spel}$ presents the main issue for the extraction of a regional climate signal, especially over the Holocene. Encouraging results can be obtained through the use of statistical methods, which allow the extraction of regional climate modes.

The SISAL database provides an excellent tool for the intercomparison of $\delta^{18}O_{spel}$ records over the Western European region. We believe this will provide an important resource of palaeoclimatic input for modelling studies and improve our understanding of the speleothem archive at mid-latitude regions.

Author Contributions: All authors contributed in the collection of data and liaison with authors of the original studies included here. F.A.L. coordinated the study, wrote the manuscript, and drafted figures 6, 7, 8. S.A.M. drafted figure 2. A.C. drafted section 3.2. and figure 3. L.C.-B. drafted figures 4 and 5. I.L. drafted section 3.3. C.P.-M. drafted sections 3.4 and 3.5. K.R. did the statistical analysis of records shown in figure 8. All authors contributed to the project, discussed manuscript ideas and edited earlier manuscript versions, and approved the final manuscript.

Funding: FAL acknowledges funding by the Swiss National Science Foundation (SNSF) grant P2EZP2_172213. SAM and LCB acknowledge funding from the Geological Survey Ireland (Short Call 2017; grant number 2017-SC-056). CP acknowledges funding by the Government of Aragón predoctoral research grant B158/13 and CGL2016-77479-R (SPYRIT) project. KR acknowledges financial support by the German Research Foundation (DFG) grant RE3994-1/1.

Acknowledgments: We thank everybody involved in SISAL for fruitful discussions and collaboration on the preparation of this manuscript. SISAL is a working group of the Past Global Changes (PAGES) programme and we thank PAGES for their support of this activity. We are grateful to Sandy Harrison for detailed and constructive criticism and editorial handling of the manuscript. We thank the World Karst Aquifer Mapping project (WOKAM) team for providing us with the karst region map presented in Figure 1.

Conflicts of Interest: The authors declare no conflict of interest. The funders had no role in the design of the study; in the collection, analyses, or interpretation of data; in the writing of the manuscript, and in the decision to publish the results.

References

[1] Atsawawanunt, K., Comas-bru, L., Mozhdehi, S.A., Deininger, M., Harrison, S.P., Baker, A., et al. (2018) The SISAL database: a global resource to document oxygen and carbon isotope records from speleothems. *Earth System Science Data Discussions*.

[2] Wong, C.I. and Breecker, D.O. (2015) Advancements in the use of speleothems as climate archives. *Quaternary Science Reviews*. 127 1–18.

[3] Henderson, G.M. (2006) Caving in to new chronologies. *Science (New York, N.Y.)*. 313 (5787), 620–622.

[4] Duplessy, J.C., Labeyrie, J., Lalou, C., and Nguyen, H. V. (1970) Continental climatic variations between 130,000 and 90,000 years BP. *Nature*. 226 631–633.

[5] Lauritzen, S.-E. and Lundberg, J. (1999) Speleothems and climate: a special issue of The Holocene. *The Holocene*. 9 (6), 643–647.

[6] McDermott, F. (2004) Palaeo-climate reconstruction from stable isotope variations in speleothems: A review. *Quaternary Science Reviews*. 23 (7–8), 901–918.

[7] Lachniet, M.S. (2009) Climatic and environmental controls on speleothem oxygen-isotope values. *Quaternary Science Reviews*. 28 (5–6), 412–432.

[8] McDermott, F., Atkinson, T.C., Fairchild, I.J., Baldini, L.M., and Mattey, D.P. (2011) A first evaluation of the spatial gradients in δ18O recorded by European Holocene speleothems. *Global and Planetary Change*. 79 (3–4), 275–287.

[9] Wassenburg, J.A., Dietrich, S., Fietzke, J., Fohlmeister, J., Jochum, K.P., Scholz, D., et al. (2016) Reorganization of the North Atlantic Oscillation during early Holocene deglaciation. *Nature Geoscience*. 9 (8), 602–605.

[10] Pérez-Mejías, C., Moreno, A., Sancho, C., Bartolomé, M., Stoll, H., Cacho, I., et al. (2017) Abrupt climate changes during Termination III in Southern Europe. *Proceedings of the National Academy of Sciences*. 114 (38), 10047–10052.

[11] IAEA/WMO (2018) Global Network of Isotopes in Precipitation. The GNIP Database. Accessible at: https://nucleus.iaea.org/wiser.

[12] Genty, D. (2008) Palaeoclimate Research in Villars Cave (Dordogne, SW-France). *International Journal of Speleology*. 37 173–191.

[13] Spötl, C., Fairchild, I.J., and Tooth, A.F. (2005) Cave air control on dripwater geochemistry, Obir Caves (Austria): Implications for speleothem deposition in dynamically ventilated caves. *Geochimica et Cosmochimica Acta*. 69 (10), 2451–2468.

[14] Sundqvist, H.S., Seibert, J., and Holmgren, K. (2007) Understanding conditions behind speleothem formation in Korallgrottan, northwestern Sweden. *Journal of Hydrology*. 347 (1–2), 13–22.

[15] Genty, D., Labuhn, I., Hoffmann, G., Danis, P.A., Mestre, O., Bourges, F., et al. (2014) Rainfall and cave water isotopic relationships in two South-France sites. *Geochimica et Cosmochimica Acta*. 131 323–343.

[16] Riechelmann, S., Schröder-Ritzrau, A., Spötl, C., Riechelmann, D.F.C., Richter, D.K., Mangini, A., et al. (2017) Sensitivity of Bunker Cave to climatic forcings highlighted through multi-annual monitoring of rain-, soil-, and dripwaters. *Chemical Geology*. 449 194–205.

[17] Kottek, M., Grieser, J., Beck, C., Rudolf, B., and Rubel, F. (2006) World map of the Köppen-Geiger

climate classification updated. *Meteorologische Zeitschrift*. 15 (3), 259–263.

[18] Geiger, R. (1961) Überarbeitete Neuausgabe von Geiger, R. in: Köppen-Geiger/Klima Der Erde. (Wandkarte 116 Mill), Klett-Perthes, Gotha, .

[19] Geiger, R. (1954) Klassifikation der klimate nach W. Köppen. in: Landolt-Börnstein, Zahlenwerte Und Funktionen Aus Phys. Chemie, Astron. Geophys. Und Tech. Alte Ser. Vol 3, .

[20] Rozanski, K., Araguás-Araguás, L., and Gonfiantini, R. (1993) Isotopic patterns in modern global precipitation. in: P.K. Swart, K.C. Lohmann, J. McKenzie, S. Savin (Eds.), Clim. Chang. Cont. Isot. Rec., AGU, pp. 1–36.

[21] Celle-Jeanton, H., Travi, Y., and Blavoux, B. (2001) Isotopic typology of the precipitation in the Western Mediterranean Region at three different time scales. *Geophysical Research Letters*. 28 (7), PP. 1215-1218.

[22] Flaim, G., Camin, F., Tonon, A., and Obertegger, U. (2013) Stable isotopes of lakes and precipitation along an altitudinal gradient in the Eastern Alps. *Biogeochemistry*. 116 187–198.

[23] Hurrell, J.W. and Deser, C. (2009) North Atlantic climate variability: The role of the North Atlantic Oscillation. *Journal of Marine Systems*. 78 (1), 28–41.

[24] Marshall, J., Kushnir, Y., Battisti, D., Chang, P., Czaja, A., Dickson, R., et al. (2001) North Atlantic climate variability: Phenomena, impacts and mechanisms. *International Journal of Climatology*. 21 (15), 1863–1898.

[25] Casty, C., Wanner, H., Luterbacher, J., Esper, J., and Böhm, R. (2005) Temperature and precipitation variability in the European Alps since 1500. *International Journal of Climatology*. 25 (14), 1855–1880.

[26] Fischer, M.J. and Mattey, D. (2012) Climate variability and precipitation isotope relationships in the Mediterranean region. *Journal of Geophysical Research Atmospheres*. 117 (20), 1–13.

[27] Baldini, L.M., McDermott, F., Foley, A.M., and Baldini, J.U.L. (2008) Spatial variability in the European winter precipitation d18O-NAO relationship: Implications for reconstructing NAO-mode climate variability in the Holocene. *Geophysical Research Letters*.

[28] Comas-Bru, L., McDermott, F., and Werner, M. (2016) The effect of the East Atlantic pattern on the precipitation δ18O-NAO relationship in Europe. *Climate Dynamics*. 47 (7–8), 2059–2069.

[29] Deininger, M., McDermott, F., Mudelsee, M., Werner, M., Frank, N., and Mangini, A. (2017) Coherency of late Holocene European speleothem δ18O records linked to North Atlantic Ocean circulation. *Climate Dynamics*. 49 (1–2), 595–618.

[30] Langebroek, P.M., Werner, M., and Lohmann, G. (2011) Climate information imprinted in oxygen-isotopic composition of precipitation in Europe. *Earth and Planetary Science Letters*. 311 (1–2), 144–154.

[31] Field, R.D. (2010) Observed and modeled controls on precipitation δ18O over Europe: From local temperature to the Northern Annular Mode. *Journal of Geophysical Research Atmospheres*. 115 (12),.

[32] Moore, G.W.K., Pickart, R.S., and Renfrew, I.A. (2011) Complexities in the climate of the subpolar North Atlantic: A case study from the winter of 2007. *Quarterly Journal of the Royal Meteorological Society*. 137 (656), 757–767.

[33] Moore, G.W.K., Renfrew, I.A., and Pickart, R.S. (2013) Multidecadal mobility of the north atlantic oscillation. *Journal of Climate*. 26 (8), 2453–2466.

[34] Comas-Bru, L. and McDermott, F. (2014) Impacts of the EA and SCA patterns on the European twentieth century NAO-winter climate relationship. *Quarterly Journal of the Royal Meteorological Society*. 140 (679), 354–363.

[35] Martin-Vide, J. and Lopez-Bustins, J.-A. (2006) The Western Mediterranean Oscillation and rainfall in the Iberian Peninsula. *International Journal of Climatology*. 26 1455–1475.

[36] Chen, Z., Auler, A.S., Bakalowicz, M., Drew, D., Griger, F., Hartmann, J., et al. (2017) The World Karst

Aquifer Mapping project: concept, mapping procedure and map of Europe. *Hydrogeology Journal*. 25 771–785.

[37] Drysdale, R.N., Zanchetta, G., Hellstrom, J.C., Fallick, A.E., Zhao, J.X., Isola, I., et al. (2004) Palaeoclimatic implications of the growth history and stable isotope (d18O and d13C) geochemistry of a Middle to Late Pleistocene stalagmite from central-western Italy. *Earth and Planetary Science Letters*. 227 215–229.

[38] Drysdale, R.N., Zanchetta, G., Hellstrom, J.C., Fallick, A.E., and Zhao, J.X. (2005) Stalagmite evidence for the onset of the Last Interglacial in southern Europe at 129 +/- 1 ka. *Geophysical Research Letters*. 32 (24), 1–4.

[39] Mattey, D., Lowry, D., Duffet, J., Fisher, R., Hodge, E., and Frisia, S. (2008) A 53 year seasonally resolved oxygen and carbon isotope record from a modern Gibraltar speleothem: Reconstructed drip water and relationship to local precipitation. *Earth and Planetary Science Letters*. 269 (1–2), 80–95.

[40] Scholz, D., Frisia, S., Borsato, A., Spötl, C., Fohlmeister, J., Mudelsee, M., et al. (2012) Holocene climate variability in north-eastern Italy: Potential influence of the NAO and solar activity recorded by speleothem data. *Climate of the Past*. 8 (4), 1367–1383.

[41] Linge, H., Lauritzen, S.-E., and Lundberg, J. (2001) Stable isotope stratigraphy of a late Last Interglacial speleothem from Rana, Northern Norway. *Quaternary Research*. 56 (2), 155–164.

[42] Berstad, I.M., Lundberg, J., Lauritzen, S.E., and Linge, H. (2002) Comparison of the climate during marine isotope stage 9 and 11 inferred from a speleothem isotope record from northern Norway. *Quaternary Research*. 58 (3), 361–371.

[43] Lauritzen, S.-E. and Lundberg, J. (2004) Isotope Stage 11, the "Super-Interglacial", from a north Norwegian speleothem. in: Stud. Cave Sediments, Springer, Boston, MApp. 257–272.

[44] Scroxton, N., Gagan, M.K., Dunbar, G.B., Ayliffe, L.K., Hantoro, W.S., Shen, C.C., et al. (2016) Natural attrition and growth frequency variations of stalagmites in southwest Sulawesi over the past 530,000 years. *Palaeogeography, Palaeoclimatology, Palaeoecology*. 441 823–833.

[45] Lisiecki, L.E. and Raymo, M.E. (2005) A Pliocene-Pleistocene stack of 57 globally distributed benthic d18O records. *Paleoceanography*. 20 (1), 1–17.

[46] Genty, D., Blamart, D., Ouahdi, R., Gilmour, M., Baker, A., Jouzel, J., et al. (2003) Precise dating of Dansgaard-Oeschger climate oscillations in western Europe from stalagmite data. *Nature*. 421 (6925), 833–837.

[47] Genty, D., Combourieu-Nebout, N., Peyron, O., Blamart, D., Wainer, K., Mansuri, F., et al. (2010) Isotopic characterization of rapid climatic events during OIS3 and OIS4 in Villars Cave stalagmites (SW-France) and correlation with Atlantic and Mediterranean pollen records. *Quaternary Science Reviews*. 29 (19–20), 2799–2820.

[48] Genty, D., Blamart, D., Ghaleb, B., Plagnes, V., Causse, C., Bakalowicz, M., et al. (2006) Timing and dynamics of the last deglaciation from European and North African δ13C stalagmite profiles-comparison with Chinese and South Hemisphere stalagmites. *Quaternary Science Reviews*. 25 2118–2142.

[49] Wainer, K., Genty, D., Blamart, D., Hoffmann, D., and Couchoud, I. (2009) A new stage 3 millennial climatic variability record from a SW France speleothem. *Palaeogeography, Palaeoclimatology, Palaeoecology*. 271 (1–2), 130–139.

[50] Wainer, K., Genty, D., Blamart, D., Daëron, M., Bar-Matthews, M., Vonhof, H., et al. (2011) Speleothem record of the last 180 ka in Villars cave (SW France): Investigation of a large δ18O shift between MIS6 and MIS5. *Quaternary Science Reviews*. 30 (1–2), 130–146.

[51] Labuhn, I., Genty, D., Vonhof, H., Bourdin, C., Blamart, D., Douville, E., et al. (2015) A high-resolution fluid inclusion δ18O record from a stalagmite in SW France: modern calibration and comparison with multiple proxies. *Quaternary Science Reviews*. 110 152–165.

[52] Atkinson, T.C. and Hopley, P.J. (2013) Speleothems and Palaeoclimates. in: Caves Karst Yorksh. Dales, Wiley-Blackwell, Buxtonpp. 181–186.

[53] Boch, R., Cheng, H., Spötl, C., Edwards, R.L., Wang, X., and Häuselmann, P. (2011) NALPS: A precisely dated European climate record 120-60 ka. *Climate of the Past*. 7 (4), 1247–1259.

[54] Genty, D., Massault, M., Gilmour, M., Baker, A., Verheyden, S., and Kepens, E. (1999) Calculations of past dead carbon proportion and variability by the comparison of AMS 14C and TIMS U/Th ages on two Holocene stalagmites. *Radiocarbon*. 41 (3), 251–270.

[55] Genty, D., Vokal, B., Obelic, B., and Massault, M. (1998) Bomb 14 C time history recorded in two modern stalagmites — importance for soil organic matter dynamics and bomb 14 C distribution over continents. *Earth and Planetary Science Letters*. 160 (160), 795–809.

[56] Vansteenberge, S., Verheyden, S., Cheng, H., Edwards, L.R., Keppens, E., and Claeys, P. (2016) Paleoclimate in continental northwestern Europe during the Eemian and early Weichselian (125-97 ka): insights from a Belgian speleothem. *Climate of the Past Discussions*. 1–22.

[57] Baker, A., Wilson, R., Fairchild, I.J., Franke, J., Spötl, C., Mattey, D., et al. (2011) High resolution δ18O and δ13C records from an annually laminated Scottish stalagmite and relationship with last millennium climate. *Global and Planetary Change*. 79 (3–4), 303–311.

[58] Baker, A., Bradley, C., Phipps, S.J., Fischer, M., Fairchild, I.J., Fuller, L., et al. (2012) Millennial-length forward models and pseudoproxies of stalagmite δ18O: An example from NW Scotland. *Climate of the Past*. 8 (4), 1153–1167.

[59] Linge, H., Lauritzen, S.E., Andersson, C., Hansen, J.K., Skoglund, R.O., and Sundqvist, H.S. (2009) Stable isotope records for the last 10 000 years from Okshola cave (Fauske, northern Norway) and regional comparisons. *Clim. Past*. 5 (4), 667–682.

[60] Ponte, J.M., Font, E., Veiga-Pires, C., Hillaire-Marcel, C., and Ghaleb, B. (2017) The effect of speleothem surface slope on the remanent magnetic inclination. *Journal of Geophysical Research: Solid Earth*. 122 (6), 4143–4156.

[61] Sundqvist, H.S., Holmgren, K., and Lauritzen, S.-E. (2007) Stable isotope variations in stalagmites from northwestern Sweden document climate and environmental changes during the early Holocene. *The Holocene*. 17 (2), 259–267.

[62] Linge, H., Baker, A., Andersson, C., and Lauritzen, S.E. (2009) Variability in luminescent lamination and initial230Th/232Th activity ratios in a late Holocene stalagmite from northern Norway. *Quaternary Geochronology*. 4 (3), 181–192.

[63] Daley, T.J., Thomas, E.R., Holmes, J.A., Street-Perrott, F.A., Chapman, M.R., Tindall, J.C., et al. (2011) The 8200yr BP cold event in stable isotope records from the North Atlantic region. *Global and Planetary Change*. 79 (3–4), 288–302.

[64] Luetscher, M., Boch, R., Sodemann, H., Spötl, C., Cheng, H., Edwards, R.L., et al. (2015) North Atlantic storm track changes during the Last Glacial Maximum recorded by Alpine speleothems. *Nature Communications*. 6 6344.

[65] Fohlmeister, J., Vollweiler, N., Spötl, C., and Mangini, A. (2012) COMNISPA II : Update of a mid-European isotope climate record , 11 ka to present.

[66] Couchoud, I., Genty, D., Hoffmann, D., Drysdale, R., and Blamart, D. (2009) Millennial-scale climate

variability during the Last Interglacial recorded in a speleothem from south-western France. *Quaternary Science Reviews*. 28 (27–28), 3263–3274.

[67] Moreno, A., Stoll, H., Jiménez-Sánchez, M., Cacho, I., Valero-Garcés, B., Ito, E., et al. (2010) A speleothem record of glacial (25-11.6 kyr BP) rapid climatic changes from northern Iberian Peninsula. *Global and Planetary Change*. 71 (3–4), 218–231.

[68] Rudzka, D., McDermott, F., Baldini, L.M., Fleitmann, D., Moreno, A., and Stoll, H. (2011) The coupled d13C-radiocarbon systematics of three Late Glacial/early Holocene speleothems; insights into soil and cave processes at climatic transitions. *Geochimica et Cosmochimica Acta*. 75 (15), 4321–4339.

[69] Mattey, D.P., Fairchild, I.A.N.J., Atkinson, T.I.M.C., Latin, J., Ainsworth, M., and Durell, R. (2010) Seasonal microclimate control of calcite fabrics, stable isotopes and trace elements in modern speleothem from St Michaels Cave, Gibraltar. in: H.M. Pedley, M. Rogerson (Eds.), Tufas Speleothems Unravelling Microb. Phys. Control., Special pu, Geological Society of London, Londonpp. 323–344.

[70] Baldini, J.U.L. (2001) Morphologic and dimensional linkage between recently deposited speleothems and drip water from Browns Folly Mine, Wiltshire, England. *Journal of Cave and Karst Studies*. 63 (3), 83–90.

[71] Baldini, J.U.L., McDermott, F., Baker, a., Baldini, L.M., Mattey, D.P., and Railsback, L.B. (2005) Biomass effects on stalagmite growth and isotope ratios: A 20th century analogue from Wiltshire, England. *Earth and Planetary Science Letters*. 240 (2), 486–494.

[72] Columbu, A., Drysdale, R., Capron, E., Woodhead, J., De Waele, J., Sanna, L., et al. (2017) Early last glacial intra-interstadial climate variability recorded in a Sardinian speleothem. *Quaternary Science Reviews*. 169 391–397.

[73] McDermott, F., Frisia, S., Huang, Y., Longinelli, A., Spiro, B., Heaton, T.H.E., et al. (1999) Holocene climate variability in Europe: Evidence from d18O, textural and extension-rate variations in three speleothems. *Quaternary Science Reviews*. 18 (8–9), 1021–1038.

[74] McDermott, F., Mattey, D.P., and Hawkesworth, C. (2001) Centennial-scale holocene climate variability revealed by a high-resolution speleothemd18O record from SW Ireland. *Science*. 294 (5545), 1328–1331.

[75] Boch, R., Spötl, C., and Kramers, J. (2009) High-resolution isotope records of early Holocene rapid climate change from two coeval stalagmites of Katerloch Cave, Austria. *Quaternary Science Reviews*. 28 (23–24), 2527–2538.

[76] Boch, R. and Spötl, C. (2011) Reconstructing palaeoprecipitation from an active cave flowstone. *Journal of Quaternary Science*.

[77] Sundqvist, H.S., Holmgren, K., Moberg, A., Spötl, C., and Mangini, A. (2010) Stable isotopes in a stalagmite from NW Sweden document environmental changes over the past 4000 years. *Boreas*. 39 77–86.

[78] Moseley, G.E., Spötl, C., Cheng, H., Boch, R., Min, A., and Edwards, R.L. (2015) Termination-II interstadial/stadial climate change recorded in two stalagmites from the north European Alps. *Quaternary Science Reviews*. 127 229–239.

[79] Bartolomé, M., Moreno, A., Sancho, C., Stoll, H.M., Cacho, I., Spötl, C., et al. (2015) Hydrological change in Southern Europe responding to increasing North Atlantic overturning during Greenland Stadial 1. *Proceedings of the National Academy of Sciences of the United States of America*. 112 (28), 6568–6572.

[80] Plagnes, V., Causse, C., Genty, D., Paterne, M., and Blamart, D. (2002) A discontinuous climatic record from 187 to 74 ka from a speleothem of the Clamouse Cave (south of France). *Earth and Planetary Science Letters*. 201 (1), 87–103.

[81] Moreno, A., Pérez-Mejías, C., Bartolomé, M., Sancho, C., Cacho, I., Stoll, H., et al. (2017) New speleothem data from Molinos and Ejulve caves reveal Holocene hydrological variability in northeast Iberia. *Quaternary Research*. 1–11.

[82] Munoz, A., Bartolome, M., Munoz, A., Sancho, C., Moreno, A., Hellstrom, J.C., et al. (2015) Solar influence and hydrological variability during the Holocene from a speleothem annual record (Molinos Cave, NE Spain). *Terra Nova*. 27 (4), 300–311.

[83] Moseley, G.E., Spötl, C., Svensson, A., Cheng, H., Brandstätter, S., and Edwards, R.L. (2014) Multi-speleothem record reveals tightly coupled climate between central europe and greenland during marine isotope stage 3. *Geology*. 42 (12), 1043–1046.

[84] Fohlmeister, J., Schröder-Ritzrau, A., Scholz, D., Spötl, C., Riechelmann, D.F.C., Mudelsee, M., et al. (2012) Bunker cave stalagmites: an archive for central European Holocene climate variability. *Climate of the Past*. 8 1751–1764.

[85] Smith, A.C., Wynn, P.M., Barker, P.A., Leng, M.J., Noble, S.R., and Tych, W. (2016) North Atlantic forcing of moisture delivery to Europe throughout the Holocene. *Scientific Reports*. 6 (April), 24745.

[86] Meyer, M.C., Spötl, C., and Mangini, A. (2008) The demise of the Last Interglacial recorded in isotopically dated speleothems from the Alps. *Quaternary Science Reviews*. 27 (5–6), 476–496.

[87] Luetscher, M., Hoffmann, D.L., Frisia, S., and Spötl, C. (2011) Holocene glacier history from alpine speleothems, Milchbach cave, Switzerland. *Earth and Planetary Science Letters*. 302 (1–2), 95–106.

[88] Häuselmann, A.D., Fleitmann, D., Cheng, H., Tabersky, D., Günther, D., and Edwards, R.L. (2015) Timing and nature of the penultimate deglaciation in a high alpine stalagmite from Switzerland. *Quaternary Science ReviewsQuaternary Science Reviews*. 126 264–275.

[89] Spötl, C., Scholz, D., and Mangini, A. (2008) A terrestrial U/Th-dated stable isotope record of the Penultimate Interglacial. *Earth and Planetary Science Letters*. 276 (3–4), 283–292.

[90] Frisia, S., Borsato, A., Mangini, A., Spötl, C., Madonia, G., and Sauro, U. (2006) Holocene climate variability in Sicily from a discontinuous stalagmite record and the Mesolithic to Neolithic transition. *Quaternary Research*. 66 (3), 388–400.

[91] Madonia, G., Frisia, S., Borsato, A., Macaluso, T., Mangini, A., Paladini, M., et al. (2005) La Grotta di Carburangeli – ricostruzione climatica dell ' Olocene per la piana costiera della Sicilia nord-occidentale. *Studi Trent.Sci.Nat., Acta Geol.* 80 (2003), 153–167.

[92] Spötl, C., Mangini, A., and Richards, D.A. (2006) Chronology and paleoenvironment of Marine Isotope Stage 3 from two high-elevation speleothems, Austrian Alps. *Quaternary Science Reviews*. 25 (9–10), 1127–1136.

[93] Drysdale, R., Zanchetta, G., Hellstrom, J., Maas, R., Fallick, A., Pickett, M., et al. (2006) Late Holocene drought responsible for the collapse of Old World civilizations is recorded in an Italian cave flowstone. *Geology*. 34 (2), 101–104.

[94] Zanchetta, G., Regattieri, E., Isola, I., Drysdale, R.N., Bini, M., Baneschi, I., et al. (2016) The so-called "4.2 event" in the central mediterranean and its climatic teleconnections. *Alpine and Mediterranean Quaternary*. 29 (1), 5–17.

[95] Railsback, L.B., Liang, F., Vidal Romaní, J.R., Grandal-d'Anglade, A., Vaqueiro Rodríguez, M., Santos Fidalgo, L., et al. (2011) Petrographic and isotopic evidence for Holocene long-term climate change and shorter-term environmental shifts from a stalagmite from the Serra do Courel of northwestern Spain, and implications for climatic history across Europe and the Mediterranean. *Palaeogeography, Palaeoclimatology, Palaeoecology*. 305 (1–4), 172–184.

[96] Drysdale, R.N., Zanchetta, G., Hellstrom, J.C., Fallick, A.E., McDonald, J., and Cartwright, I. (2007) Stalagmite evidence for the precise timing of North Atlantic cold events during the early last glacial. *Geology*. 35 (1), 77–80.

[97] Drysdale, R.N., Hellstrom, J.C., Zanchetta, G., Fallick, A.E., Sanchez Goni, M.F., Couchoud, I., et al. (2009) Evidence for obliquity forcing of Glacial Termination II. *Science (New York, N.Y.)*. 325 1527–1531.

[98] González-Lemos, S., Müller, W., Pisonero, J., Cheng, H., Edwards, R.L., and Stoll, H.M. (2015) Holocene flood frequency reconstruction from speleothems in northern Spain. *Quaternary Science Reviews*. 127 129–140.

[99] Martín-Chivelet, J., Muñoz-García, M.B., Edwards, R.L., Turrero, M.J., and Ortega, A.I. (2011) Land surface temperature changes in Northern Iberia since 4000yrBP, based on δ13C of speleothems. *Global and Planetary Change*. 77 (1–2), 1–12.

[100] Baldini, L., Mcdermott, F., Cabal, P.A., Garcia-monco, C., and Baldini, J. (2010) Climate in northern Spain through the Younger Dryas and Holocene preserved in a precisely dated speleothem from La Garma cave , Cantabria.

[101] Comas-Bru, L., McDermott, F., and Fleitmann, D. (2012) A 1,000 year annually resolved record of speleothem δ18O from Northern Spain ; a potential new proxy for North Atlantic Oscillation (NAO) index reconstruction. in: Geophys. Res. Abstr. - EGU Gen. Assem. 2012, .

[102] Domínguez-Villar, D., Wang, X., Krklec, K., Cheng, H., and Edwards, R.L. (2017) The control of the tropical North Atlantic on Holocene millennial climate oscillations. *Geology*. 45 (4), 303–306.

[103] Daëron, M., Guo, W., Eiler, J., Genty, D., Blamart, D., Boch, R., et al. (2011) 13C18O clumping in speleothems: Observations from natural caves and precipitation experiments. *Geochimica et Cosmochimica Acta*. 75 (12), 3303–3317.

[104] Genty, D., Plagnes, V., Causse, C., Cattani, O., Stievenard, M., Falourd, S., et al. (2002) Fossil water in large stalagmite voids as a tool for paleoprecipitation stable isotope composition reconstitution and paleotemperature calculation. *Chemical Geology*. 184 (1–2), 83–95.

[105] Hodge, E.J., Richards, D. a., Smart, P.L., Andreo, B., Hoffmann, D.L., Mattey, D.P., et al. (2008) Effective precipitation in southern Spain (~ 266 to 46 ka) based on a speleothem stable carbon isotope record. *Quaternary Research*. 69 (3), 447–457.

[106] Hodge, E.J., Richards, D.A., Smart, P.L., Gines, A., and Mattey, D.P. (2008) Sub-millennial climate shifts in the western Mediterranean during the last glacial period recorded in a speleothem from Mallorca, Spain. *Journal of Quaternary Science*. 23 (8), 713–718.

[107] Van Rampelbergh, M., Verheyden, S., Allan, M., Quinif, Y., Cheng, H., Edwards, L.R., et al. (2015) A 500-year seasonally resolved δ18O and δ13C, layer thickness and calcite aspect record from a speleothem deposited in the Han-sur-Lesse cave, Belgium. *Climate of the Past*. 11 (6), 789–802.

[108] Verheyden, S., Keppens, E., Strydonck, M. Van, and Quinif, Y. (2012) The 8.2 ka event: its it registered in Belgian speleothems? *Speleogenesis and Evolution of Karst Aquifers*. (12),.

[109] Verheyden, S., Keppens, E., Quinif, Y., Cheng, H., and Edwards, L.. (2014) Late-glacial and Holocene climate reconstruction as inferred from a stalagmite - Grotte du Pere Noel, Han-sur-Lesse, Belgium. *Geol.Belg*. 17 83–89.

[110] Niggemann, S., Mangini, A., Richter, D.K., and Wurth, G. (2003) A paleoclimate record of the last 17,600 years in stalagmites from the B7 cave, Sauerland, Germany. *Quaternary Science Reviews*. 22 (5–7), 555–567.

[111] Jackson, a. S., McDermott, F., and Mangini, a. (2008) Late Holocene climate oscillations and solar

fluctuations from speleothem STAL-AH-1, Sauerland, Germany: A numerical perspective. *Geophysical Research Letters*. 35 (6), 1–5.

[112] Niggemann, S., Mangini, A., Mudelsee, M., Richter, D.K., and Wurth, G. (2003) Sub-Milankovitch climatic cycles in Holocene stalagmites from Sauerland, Germany. *Earth and Planetary Science Letters*. 216 (4), 539–547.

[113] Wurth, G., Niggemann, S., Richter, D.K., and Mangini, A. (2004) The Younger Dryas and Holocene climate record of a stalagmite from Hölloch Cave(Bavarian Alps, Germany. *Journal of Quaternary Science*. 19 (3), 291–298.

[114] Zanchetta, G., Drysdale, R.N., Hellstrom, J.C., Fallick, A.E., Isola, I., Gagan, M.K., et al. (2007) Enhanced rainfall in the Western Mediterranean during deposition of sapropel S1: stalagmite evidence from Corchia cave (Central Italy). *Quaternary Science Reviews*. 26 279–286.

[115] Spötl, C. and Mangini, A. (2006) U/Th age constraints on the absence of ice in the central Inn Valley (eastern Alps, Austria) during Marine Isotope Stages 5c to 5a. *Quaternary Research*. 66 (1), 167–175.

[116] Spötl, C. and Mangini, A. (2007) Speleothems and paleoglaciers. *Earth and Planetary Science Letters*. 254 (3–4), 323–331.

[117] Cliff, R.A., Spötl, C., and Mangini, A. (2010) U-Pb dating of speleothems from Spannagel Cave, Austrian Alps: A high resolution comparison with U-series ages. *Quaternary Geochronology*. 5 (4), 452–458.

[118] Holzkamper, S., Spotl, C., and Mangini, A. (2005) High-precision constraints on timing of Alpine warm periods during the middle to late Pleistocene using speleothem growth periods. *Earth and Planetary Science Letters*. 236 (3–4), 751–764.

[119] Mangini, A., Spötl, C., and Verdes, P. (2005) Reconstruction of temperature in the Central Alps during the past 2000 yr from a d18O stalagmite record. *Earth and Planetary Science Letters*. 235 741–751.

[120] Spötl, C., Mangini, A., Frank, N., Eichstädter, R., and Burns, S.J. (2002) Start of the last interglacial period at 135 ka: Evidence from a high Alpine speleothem. *Geology*. 30 (9), 815–818.

[121] Stoykova, D., Shopov, Y., Sauro, U., Borsato, A., Cucchi, F., and Forti, P. (2003) High-Resolution Climate Proxy Records for the Last 2000 Years from a Speleothem from Savi Cave, Trieste, NE Italy. *Studi Trent.Sci.Nat., Acta Geol.* 80 (2003), 169–173.

[122] Boch, R., Spötl, C., and Frisia, S. (2011) Origin and palaeoenvironmental significance of lamination in stalagmites from Katerloch Cave, Austria. *Sedimentology*.

[123] Cheng, H., Lawrence Edwards, R., Shen, C.C., Polyak, V.J., Asmerom, Y., Woodhead, J., et al. (2013) Improvements in 230Th dating, 230Th and 234U half-life values, and U-Th isotopic measurements by multi-collector inductively coupled plasma mass spectrometry. *Earth and Planetary Science Letters*.

[124] Cheng, H., Edwards, R.L., Hoff, J., Gallup, C.D., Richards, D.A., and Asmerom, Y. (2000) The half-lives of uranium-234 and thorium-230. *Chemical Geology*. 169 17–33.

[125] Edwards, R.L., Chen, J.H., and Wasserburg, G.J. (1987) U-238-U-234-Th-230-Th-232 systematics and the precise measurement of time over the past 500,000 years. *Earth and Planetary Science Letters*. 81 175–192.

[126] Baker, A., C. Hellstrom, J., Kelly, B.F.J., Mariethoz, G., and Trouet, V. (2015) A composite annual-resolution stalagmite record of North Atlantic climate over the last three millennia. *Scientific Reports*. 5 (April), 10307.

[127] Hua, Q., McDonald, J., Redwood, D., Drysdale, R., Lee, S., Fallon, S., et al. (2012) Robust chronological reconstruction for young speleothems using radiocarbon. *Quaternary Geochronology*. 14 67–80.

[128] Shen, C.-C., Lin, K., Duan, W., Jiang, X., Partin, J.W., Edwards, R.L., et al. (2013) Testing the annual nature of speleothem banding. *Scientific Reports*. 3 (September 2003), 2633.

[129] Domínguez-Villar, D., Baker, A., Fairchild, I.J., and Edwards, R.L. (2012) A method to anchor floating chronologies in annually laminated speleothems with U-Th dates. *Quaternary Geochronology*. 14 57–66.

[130] Scholz, D. and Hoffmann, D.L. (2011) StalAge - An algorithm designed for construction of speleothem age models. *Quaternary Geochronology*. 6 (3–4), 369–382.

[131] Bronk Ramsey, C. (2008) Deposition models for chronological records. *Quaternary Science Reviews*.

[132] Bajo, P., Hellstrom, J., Frisia, S., Drysdale, R., Black, J., Woodhead, J., et al. (2016) "Cryptic" diagenesis and its implications for speleothem geochronologies. *Quaternary Science Reviews*. 148 17–28.

[133] Railsback, L.B., Dabous, A.A., Osmond, J.K., and Fleisher, C.J. (2002) Petrographic and geochemical screening of speleothems for U-series dating: An example from recrystallized speleothems from Wadi Sannur Cavern, Egypt. *Journal of Cave and Karst Studies*. 64 (2), 108–116.

[134] De Waele, J., D'Angeli, I.M., Bontognali, T., Tuccimei, P., Scholz, D., Jochum, K.P., et al. (2018) Speleothems in a north Cuban cave register sea level changes and Pleistocene uplift rates. *Earth Surface Processes and Landforms*. accepted.

[135] Scholz, D., Tolzmann, J., Hoffmann, D.L., Jochum, K.P., Spötl, C., and Riechelmann, D.F.C. (2014) Diagenesis of speleothems and its effect on the accuracy of230Th/U-ages. *Chemical Geology*. 387 (1), 74–86.

[136] Scholz, D., Hoffmann, D.L., Hellstrom, J., and Bronk Ramsey, C. (2012) A comparison of different methods for speleothem age modelling. *Quaternary Geochronology*. 14 94–104.

[137] van der Meulen, J.P. and Brandsma, T. (2008) Thermometer screen intercomparison in De Bilt (The Netherlands), Part I: Understanding the weather-dependent temperature differences). *International Journal of Climatology*. 28 (3), 371–387.

[138] Parker, D.E., Legg, T.P., and Folland, C.K. (1992) A new daily central England temperature series, 1772–1991. *International Journal of Climatology*. 12 (4), 317–342.

[139] Moberg, A., Bergström, H., Ruiz Krigsman, J., and Svanered, O. (2002) Daily air temperature and pressure series for Stockholm (1756-1998). *Climatic Change*. 53 (1), 171–212.

[140] Harris, I., Jones, P.D., Osborn, T.J., and Lister, D.H. (2013) Updated high-resolution grids of monthly climatic observations - the CRU TS3.10 Dataset. *International Journal of Climatology*. 34 (3), 623–642.

[141] Fuller, L., Baker, A., Fairchild, I.J., Spötl, C., Marca-Bell, A., Rowe, P., et al. (2008) Isotope hydrology of dripwaters in a Scottish cave and implications for stalagmite palaeoclimate research. *Hydrology and Earth System Sciences*. 12 (4), 1065–1074.

[142] Mischel, S.A., Scholz, D., and Spötl, C. (2015) δ18O values of cave drip water: a promising proxy for the reconstruction of the North Atlantic Oscillation? *Climate Dynamics*. 45 (11–12), 3035–3050.

[143] Tan, M., Baker, A., Genty, D., Smith, C., Esper, J., and Cai, B. (2006) Applications of stalagmite laminae to paleoclimate reconstructions: Comparison with dendrochronology/climatology. *Quaternary Science Reviews*. 25 (17–18), 2103–2117.

[144] Vaks, A., Gutareva, O.S., Breitenbach, S.F.M., Avirmed, E., Mason, A.J., Thomas, A.L., et al. (2013) Speleothems Reveal 500,000-Year History of Siberian Permafrost. *Science (New York, N.Y.)*. 340 183–186.

[145] Holzkämper, S., Mangini, A., Spötl, C., and Mudelsee, M. (2004) Timing and progression of the Last Interglacial derived from a high alpine stalagmite. *Geophysical Research Letters*. 31 (7),.

[146] Dansgaard, W. (1964) Stable isotopes in precipitation. *Tellus*. 16 (4), 436–468.

[147] Moreno, A., Sancho, C., Bartolomé, M., Oliva-Urcia, B., Delgado-Huertas, A., Estrela, M.J., et al. (2014) Climate controls on rainfall isotopes and their effects on cave drip water and speleothem growth: the case of Molinos cave (Teruel, NE Spain). *Climate Dynamics*. 43 (1), 221–241.

[148] Dumitru, O.A., Onac, B.P., Polyak, V.J., Wynn, J.G., Asmerom, Y., and Fornós, J.J. (2018) Climate variability in the western Mediterranean between 121 and 67 ka derived from a Mallorcan speleothem record. *Palaeogeography, Palaeoclimatology, Palaeoecology*. in press.

[149] Laîné, A., Kageyama, M., Salas-Mélia, D., Voldoire, A., Rivièlre, G., Ramstein, G., et al. (2009) Northern hemisphere storm tracks during the last glacial maximum in the PMIP2 ocean-atmosphere coupled models: Energetic study, seasonal cycle, precipitation. *Climate Dynamics*. 32 (5), 593–614.

[150] van Breukelen, M.R., Vonhof, H.B., Hellstrom, J.C., Wester, W.C.G., and Kroon, D. (2008) Fossil dripwater in stalagmites reveals Holocene temperature and rainfall variation in Amazonia. *Earth and Planetary Science Letters*. 275 (1–2), 54–60.

[151] Bowen, G.J. and Revenaugh, J. (2003) Interpolating the isotopic composition of modern meteoric precipitation. *Water Resources Research*. 39 (10), 1–13.

[152] Kim, S.-T. and O'Neil, J.R. (1997) Equilibrium and nonequilibrium oxygen isotope effects in synthetic carbonates. *Geochimica et Cosmochimica Acta*. 61 (16), 3461–3475.

[153] Wackerbarth, A., Langebroek, P.M., Werner, M., Lohmann, G., Riechelmann, S., Borsato, A., et al. (2012) Simulated oxygen isotopes in cave drip water and speleothem calcite in European caves. *Climate of the Past*. 8 1781–1799.

[154] Rasmussen, S.O., Bigler, M., Blockley, S.P., Blunier, T., Buchardt, S.L., Clausen, H.B., et al. (2014) A stratigraphic framework for abrupt climatic changes during the Last Glacial period based on three synchronized Greenland ice-core records: Refining and extending the INTIMATE event stratigraphy. *Quaternary Science Reviews*. 106 14–28.

[155] Wolff, E.W., Chappellaz, J., Blunier, T., Rasmussen, S.O., and Svensson, A. (2010) Millennial-scale variability during the last glacial : The ice core record. *Quaternary Science Reviews*. 29 (21–22), 2828–2838.

[156] NGRIP Project Members (2004) High-resolution record of Northern Hemisphere climate extending into the last interglacial period. *Nature*. 431 (7005), 147–151.

[157] Svensson, A., Andersen, K.K., Bigler, M., Clausen, H.B., Dahl-Jensen, D., Davies, S.M., et al. (2008) A 60 000 year Greenland stratigraphic ice core chronology. *Climate of the Past*. 4 47–57.

[158] Moreno, A., Stoll, H.M., Jiménez-Sánchez, M., Cacho, I., Valero-Garcés, B., Ito, E., et al. (2010) A speleothem record of rapid climatic shifts during last glacial period from Northern Iberian Peninsula. *Global and Planetary Change*. 71 218–231; doi:10.1016/j.gloplacha.2009.10.002.

[159] Rehfeld, K., Münch, T., Ho, S.L., and Laepple, T. (2018) Global patterns of declining temperature variability from the Last Glacial Maximum to the Holocene. *Nature*. 554 (7692), 356–359.

[160] Sigl, M., Winstrup, M., Mcconnell, J.R., Welten, K.C., Plunkett, G., Ludlow, F., et al. (2015) Timing and climate forcing of volcanic eruptions for the past 2,500 years. *Nature*. 523 543–549.

[161] Steinhilber, F., Beer, J., and Fröhlich, C. (2009) Total solar irradiance during the Holocene. *Geophysical Research Letters*. 36 (19), 1–5.

[162] MacFarling Meure, C., Etheridge, D., Trudinger, C., Steele, P., Langenfelds, R., Van Ommen, T., et al. (2006) Law Dome CO2, CH4 and N2O ice core records extended to 2000 years BP. *Geophysical Research Letters*. 33 (14), 2000–2003.

[163] PAGES 2k Consortium (2013) Continental-scale temperature variability during the past two millennia. *Nature Geoscience*. 6 (April), 339–346.

[164] Mann, M.E., Zhang, Z., Rutherford, S., Bradley, R.S., Hughes, M.K., Shindell, D., et al. (2009) Global signatures and dynamical origins of the Little Ice Age and Medieval Climate Anomaly. *Science (New York, N.Y.)*. 326 (5957), 1256–1260.

[165] Büntgen, U., Myglan, V.S., Ljungqvist, F.C., Mccormick, M., Cosmo, N. Di, Sigl, M., et al. (2016) Cooling and societal change during the Late Antique Little Ice Age from 536 to around 660 AD. *Nature Geoscience*. 9 (3), 231–236.

[166] Cheng, H., Edwards, R.L., Sinha, A., Spötl, C., Yi, L., Chen, S., et al. (2016) The Asian monsoon over the past 640,000 years and ice age terminations. *Nature*. 534 640–646.

[167] Stoll, H., Perez, C., Cacho, I., Moreno, A., Iglesias, M., and Edwards, R.L. (2018) Chronlogy for deglaciation during Termination II from stalagmites in NW Spain. 20 18654.